American Journal of Botany 94(7): 1094–1115. 2007.

COMPARATIVE INFRUCTESCENCE MORPHOLOGY IN *ALTINGIA* (ALTINGIACEAE) AND DISCORDANCE BETWEEN MORPHOLOGICAL AND MOLECULAR PHYLOGENIES[1]

STEFANIE M. ICKERT-BOND,[2,3,6] KATHLEEN B. PIGG,[3] AND JUN WEN[4,5]

[2]UA Museum of the North Herbarium, Department of Biology and Wildlife, and Institute of Arctic Biology, University of Alaska Fairbanks, 907 Yukon Drive, Fairbanks, Alaska 99775-6590 USA; [3]School of Life Sciences, Box 874501, Arizona State University, Tempe, Arizona 85287-4501 USA; [4]Department of Botany, MRC-166, Smithsonian Institution, P.O. Box 37012, Washington, D.C. 20013-7012 USA; and [5]Laboratory of Systematic and Evolutionary Botany & Herbarium, Institute of Botany, Chinese Academy of Sciences, Beijing 100093, China

Altingia (Altingiaceae) is a tropical to subtropical Asian genus of lowland trees for which 5–15 species have been recognized. Morphological diversity, particularly of the mature infructescence, has been poorly known, especially for species with relatively localized and narrow distributions, and our understanding of *Altingia* has lagged behind that of its close temperate relative *Liquidambar* (sweet gum). In this contribution, mature infructescence structure, at the levels of anatomy, morphology, and micromorphology, and some distinctive inflorescence features, are described for five recognized species of *Altingia*, some for the first time. In the phylogenetic framework of both morphology and molecules, characters of *Altingia* contrast with those of *Liquidambar* and suggest that character evolution within Altingiaceae is at least partly related to geographic and climatic distribution. Differences in rates of evolution and morphological convergence suggest complex patterns of diversification in Altingiaceae at several different phylogenetic levels: (1) at the deep nodes, characters of the stem lineage fossil *Microaltingia* persist into crown group Altingiaceae, morphological stasis; (2) at the generic level, convergence within both *Liquidambar* and *Altingia* toward their respective habitats; (3) at the infrageneric level, morphological divergence in species diversification within *Altingia*, in response to diverse habitats of the eastern Asian subtropics; and (4) within the intercontinental disjunct species pair *L. orientalis–L. styraciflua*, morphological stasis.

Key words: *Altingia*; Altingiaceae; biogeography; infructescence; morphological stasis.

The genus *Altingia* Noronha (Altingiaceae) has been reported to consist of about 5–15 species occurring in tropical to subtropical regions of Asia. Two sections have been recognized traditionally: section *Oligocarpa,* including *A. gracilipes* Hemsl. and *A. siamensis* Craib; and section *Altingia*, including *A. chinensis* Oliver ex Hance, *A. obovata* Merrill & Chun, *A. yunnanensis* Rehder & Wilson, *A. poilanei* Tardieu-Blot, and *A. excelsa* Noronha (Chang, 1979; Ferguson, 1989). We recognize five of these species in the present study: *A. gracilipes*, *A. siamensis* Craib, *A. chinensis*, *A. excelsa,* and *A. poilanei* (Table 1), (Ickert-Bond et al., 2005). Several additional species that have been included within section *Altingia* by Chang (1979) are not treated here because they are poorly known, and their taxonomic status needs to be critically evaluated.

[1] Manuscript received 9 July 2006; revision accepted 21 May 2007.

The authors thank N. Aksoy (ISTO), A. L. Bogle (NHA), R. Hitchin (UWBG), S. Shi (SYS), and E. Wood (GH) for providing material for study; B. Chen (IBSC) and P. K. Loc (HNU) for assistance in the field; B. A. Strack (F) for assistance with the SEM; the curators of the following herbaria for allowing access to collections: E, F, FI, GH, HK, HN, IBSC, MO, P, PE, SYS, and XAL; and T. Yi (F), Z. Nie (KUN), and J. Wang (ASU) for Chinese translations. This study was funded by a Boyd Postdoctoral Fellowship and a grant from the Field Dreams Program, Women's Board, the Field Museum of Natural History, National Geographic Society Explorers Grant NGS-7644–04, and a generous donation by the Wallace Desert Gardens, Scottsdale, Arizona, to S.M.I.-B.; NSF EAR-9980388 and EAR-0345838 and a Minigrant, College of Liberal Arts & Sciences, Arizona State University, to K.B.P.; and NSF DEB-0108536, Department of Botany and the Laboratory of Analytical Biology of the Smithsonian Institution, and a collaborative research grant from the Institute of Botany of the Chinese Academy of Sciences, to J.W.

[6]Author for correspondence (e-mail: steffi.ickertbond@uaf.edu)

Historically, four species of *Altingia* were recognized in the early 1900s: *A. excelsa, A. chinensis*, *A. yunnanensis*, and *A. gracilipes*. *Altingia excelsa* is a widely distributed species from the Himalayas (Assam of India) eastward through Myanmar (formerly Burma), to southeastern China and south to Indochina (Thailand, Cambodia, Laos, and Vietnam), Malaysia, and Indonesia (Ferguson, 1989). *Altingia chinensis* occurs widely in China and is closely allied with specimens designated as *A. yunnanensis* from Yunnan, China, and southern Vietnam (Ferguson, 1989). In this report we consider *A. yunnanensis* to be synonymous with *A. chinensis* (Table 1). *Altingia gracilipes* occurs in Fujian, Hong Kong, Hainan, Guangdong, Jiangxi, and Zhejiang provinces and is highly distinct from the *A. chinensis–A. yunnanensis* complex in having fewer fruits and a cup-like bract that subtends each infructescence (Zhang et al., 2003).

Other species described after these initial four taxa include *Altingia siamensis* Craib, *A. obovata*, *A. angustifolia* H.-T. Chang, *A. indochinensis* H.-T. Chang, *A. multinervis* Cheng, and *A. tenuifolia* Chun ex H.-T. Chang. We recognize *A. siamensis* as a widespread species extending from northern Thailand, Cambodia, Laos and Vietnam, into eastern Guangdong, and southern Yunnan (Craib, 1928). *Altingia obovata* was described from the Hainan Island of southern China (Merrill and Chun, 1935) and was distinguished from populations of *A. chinensis* on the mainland by its obovate, rather than the typically ovate-to-elliptic, leaves. Because this character is polymorphic throughout populations of *A. chinensis* (Ferguson, 1989; S. Ickert-Bond, personal observation), we consider *A. obovata* as a synonym of *A. chinensis*.

None of the three species described by Hong-Ta Chang in the 1960s, *A. angustifolia* from Guangdong province, *A.*

TABLE 1. Taxonomy of *Altingia* species recognized in this study.

Taxon	Synonyms
Altingia chinensis (Champion ex Bentham) Oliver ex Hance	*A. chinensis* f. *pubescens* X. H. Song
	A. multinervis Cheng
	A. obovata Merrill et Chun
	A. yunnanensis Rehder & Wilson
A. excelsa Noronha	*Liquidambar altingiana* Blume
A. gracilipes Hemsl.	*A. gracilipes* Hemsl. var. *serrulata* Tutcher
	A. tenuifolia Chun ex H.-T. Chang
	A. uniflora H.-T. Chang
A. poilanei Tardieu-Blot	
A. siamensis Craib	*A. angustifolia* H.-T. Chang
	A. takhtajanii Thai
	A. tenuifolia Chun ex H.-T. Chang
Insufficient material	*A. cambodiana* Lecomte
	A. indochinensis H.-T. Chang

indochinensis from Vietnam, or *A. tenuifolia* from Guizhou province, is recognized in the present study. *Altingia angustifolia* is here treated as a synonym of *A. siamensis* (Zhang et al., 2003). *Altingia indochinensis* is a doubtful name and is taxonomically problematic without a confirmed locality, and we consider *A. tenuifolia* to be a synonym of *A. gracilipes* (S. Ickert-Bond and J. Wen, unpublished data). We recognize *A. poilanei,* a species with distinctive, broadly ovate leaves and elongate infructescences, known only from its type locality in northern Vietnam (Tardieu-Blot, 1965). *Altingia multinervis* was recognized from a single type specimen (Cheng, 1947). The first author examined an apparent isotype (*Tsoong 256*) at the Herbarium of Zhongshan (Sun Yatsen) University (SYS), which consists only of two sterile leaves (S. Ickert-Bond, personal observation). We recently obtained digital images of the holotype from the Herbarium at Nanjing University (N). This specimen includes branches as well as two badly degraded and incomplete infructescences. The lack of information, particularly about fertile remains of *A. multinervis,* prevents further consideration of this material at present. Variation seen in leaf morphology is consistent with that found in *A. chinensis*.

While *Altingia* is tropical–subtropical in distribution, its sister taxon, *Liquidambar* L., the sweet gum, is a mostly temperate taxon (Shi et al., 1998; Wen, 1998, 1999, 2001). The third genus within Altingiaceae, *Semiliquidambar* H.-T. Chang (Chang, 1962) has been hypothesized to have originated via intergeneric hybridization between *Altingia* and *Liquidambar* (Bogle, 1986; Ickert-Bond et al., 2005). This genus is restricted to subtropical and tropical Asia, especially in southern China, and is currently under study. As with *Liquidambar*, taxonomic delimitation of *Altingia* has been based largely on leaf and inflorescence morphology, and until recently, details of mature infructescences of either genus were not clearly known (Ickert-Bond et al., 2005). This situation has been even more problematic for *Altingia* because of the difficulty in obtaining material for most taxa, and a revision is in order (Endress, 1993).

As part of our broader analysis of the family Altingiaceae, we have described the silicified Miocene infructescence *Liquidambar changii* Pigg, Ickert-Bond and Wen (Pigg et al., 2004), completed a comparative study of mature infructescences of extant *Liquidambar* (Ickert-Bond et al., 2005), and investigated the complexity of the biogeographic history of the family using molecular markers (Ickert-Bond and Wen, 2006). It is clear that this family has an ancient origin, with earliest evidence of the stem lineage of Altingiaceae in the Late Cretaceous (*Microaltingia* Zhou, Crepet and Nixon; Zhou et al., 2001; Hermsen et al., 2006) and diversification throughout the Tertiary (Ferguson, 1989; Pigg et al., 2004). In this contribution we expand the morphological studies of Altingiaceae to include the genus *Altingia* and to document the diversity therein. The discrepancy between morphological and molecular rates of evolution reported in our earlier studies (Ickert-Bond et al., 2005; Ickert-Bond and Wen, 2006) is further considered to examine the patterns of character evolution and diversification within Altingiaceae in the context of geographic and climatic distribution.

MATERIALS AND METHODS

Material for study was obtained from field collections and from herbarium specimens (Table 2, Appendix); material was photographed for general features. Measurements given are the mean of 10 individuals (Table 3). Some specimens were hand-sectioned with a razor blade for general features, and examples from all species were prepared for serial section using standard histological techniques that included embedding in Paraplast Plus Tissue Embedding Medium (Monoject Scientific, Sherwood Medical, St. Louis, Missouri, USA), sectioning on a rotary microtome at 20 μm thick, and staining with standard histological stains (Johansen, 1940). Mature, woody infructescences were softened with ethylene diamine prior to embedding (Carlquist, 1982). For anatomical studies, dry seeds were rehydrated for 7 d in equal parts of glycerol, water, and ethanol and then sectioned by hand (Lobova et al.,

TABLE 2. Plant material including GenBank accession numbers used for phylogenetic analysis of molecular data from Ickert-Bond and Wen (2006), but a reduced set of taxa has been used in the current study. All voucher specimens are deposited at the Field Museum Herbarium (F).

		GenBank Accession numbers				
Taxon	Voucher	*trnL-trnF* IGS	*psa*A-*ycf3* IGS	*rps16* intron	*trn*S-*trn*G IGS	*trnG* intron
Hamamelis virginiana	*Wen 6229*	DQ352196	DQ352227	DQ352260	DQ352292	DQ35324
Exbucklandia tonkinensis	*Ickert-Bond 1269*	DQ352198	DQ352229	DQ352262	DQ352294	DQ352326
Liquidambar acalycina	*Wen 8146–11*	DQ352216	DQ352247	DQ352281	DQ352313	DQ352345
L. formosana	*Ickert-Bond 1291*	DQ352220	DQ352251	DQ352285	DQ352317	DQ352349
L. orientalis	*Aksoy 5203*	DQ352223	DQ352254	DQ352288	DQ352320	DQ352353
L. styraciflua	*Wen 7169*	DQ352217	DQ352248	DQ352282	DQ352314	DQ352346
Altingia chinensis	*Ickert-Bond 1294*	DQ352202	DQ352234	DQ352267	DQ352299	DQ352331
A. excelsa	*Widjaja s.n.*	DQ352226	DQ352257	DQ352291	DQ352323	DQ352355
A. gracilipes	*Ickert-Bond 1272*	DQ352205	DQ352237	DQ352270	DQ352302	DQ352334
A. poilanei	*Ickert-Bond 1296*	DQ352208	DQ352259	DQ352275	DQ352307	DQ352339
A. siamensis	*Ickert-Bond 1281*	DQ352212	DQ352243	DQ352277	DQ352309	DQ352341

TABLE 3. Characters studied within *Altingia* in Altingiaceae (based on 10 measurements). L = length, W = width, infr. = infructescence, Pedun. = peduncle, Ventr. = ventral, surf. = surface

	Infructescence							
Taxon	L (mm)	W (mm)	L : W	Shape	No. fruits/ infr.	Pedun. L	Pedun. W	Extrafloral
A. chinensis	18.04–24.94 ($\bar{X}$ = 21.79)	22.41–27.15 ($\bar{X}$ = 25.30)	0.75–1.00 : 1 ($\bar{X}$ = 0.862 : 1)	Subglobose	14–20 ($\bar{X}$ = 16.57)	32.14–58.05 ($\bar{X}$ = 43.29)	1.32–2.30 ($\bar{X}$ = 1.69)	Irregular, mammilate
A. excelsa	13.94–17.55 ($\bar{X}$ = 15.73)	15.65–22.22 ($\bar{X}$ = 19.03)	0.65–1.02 : 1 ($\bar{X}$ = 0.84 : 1)	Compressed globose	9–25 ($\bar{X}$ = 15.38)	22.05–38.47 ($\bar{X}$ = 29.35)	0.75–1.70 ($\bar{X}$ = 1.36)	Irregular with small spines
A. gracilipes	9.56–13.44 ($\bar{X}$ = 11.96)	11.86–16.90 ($\bar{X}$ = 14.67)	0.74–0.91 : 1 ($\bar{X}$ = 0.82 : 1)	Obconical	5–6 ($\bar{X}$ = 5.78)	14.93–28.18 ($\bar{X}$ = 22.26)	0.85–1.24 ($\bar{X}$ = 1.04)	Irregular mammilate
A. poilanei	21.91–30.98 ($\bar{X}$ = 26.84)	21.47–26.80 ($\bar{X}$ = 23.87)	0.59–0.79 : 1 ($\bar{X}$ = 1.124 : 1)	Turbinate	21–32 ($\bar{X}$ = 24.83)	20.26–31.49 ($\bar{X}$ = 24.23)	0.93–2.20 ($\bar{X}$ = 1.81)	Irregular mammilate
A. siamensis	8.70–13.48 ($\bar{X}$ = 11.27)	11.70–21.65 ($\bar{X}$ = 15.81)	0.59–0.79 : 1 ($\bar{X}$ = 0.713 : 1)	Compressed globose	6–7 ($\bar{X}$ = 6.21)	20.26–31.49 ($\bar{X}$ = 24.23)	0.93–1.20 ($\bar{X}$ = 1.08)	Irregular, with small spines

2003). Seeds and dissected carpels were mounted on stubs for scanning electron microscopy (SEM), sputter-coated with 200 Å of gold, and scanned with an Amray 1400 and an Amray 1810 SEM (KLA Tencor, Amray Division, Bedford Massachusetts, USA). Terminology follows that of Bogle (1986), Endress (1989a), and Ickert-Bond et al. (2005). Interpretation of infructescence structure in Altingiaceae was discussed in Ickert-Bond et al. (2005).

To evaluate the morphological evolution of taxa in Altingiaceae and its close relatives, we conducted a morphological cladistic analysis. We scored all potentially informative morphological characters observed for the four species of *Liquidambar*, *Altingia chinensis*, *A. excelsa, A. gracilipes. A. poilanei,* and *A. siamensis,* and two recently described fossil taxa, the Cretaceous *Microaltingia apocarpela* Zhou, Crepet & Nixon from eastern North America (Zhou et al., 2001), and the middle Miocene *L. changii* Pigg, Ickert-Bond & Wen from western North America (Pigg et al., 2004). Outgroup selection, (*Exbucklandia* and *Hamamelis*) follows that of our previous analysis (Ickert-Bond et al., 2005). *Semiliquidambar* was excluded from the analysis because of hypotheses that it originated through intergeneric hybridization (Bogle, 1986; Ferguson, 1989; Ickert-Bond et al., 2005). The Eocene fossil genus *Steinhauera* Presl (Mai, 1968; Pigg et al., 2004) was excluded because it is poorly understood and needs to be reevaluated.

We emphasized reproductive structures and expanded the data matrix used by Ickert-Bond et al. (2005). Forty-nine characters were selected on the basis of interspecific variations among the sampled taxa (Table 4). They consisted of 41 binary and seven multistate characters. All multistate characters were treated as unordered. Quantitative characters were coded following simple gap coding (Archie, 1985). Data were mainly derived from our own observations and partly from the literature, as cited under Materials and Methods in Ickert-Bond et al. (2005). We added seven characters to the annotated list of all characters from our earlier analysis (Table 2 in Ickert-Bond et al., 2005). These additional characters were character 15: pollen, (0) tricolpate, (1) polyporate; character 26: outer fruit wall, (0) little differentiation, (1) well differentiated; character 27: distribution of resin canals and fiber bundle formation in outer fruit wall, (0) dispersed throughout, (1) predominantly in outer infructescence fruit wall with arclike fiber bundles; character 33: dehiscence pattern, (0) septicidal and loculicidal, (1) septicidal and ventricidal, (2) septicidal, ventricidal, and loculicidal; character 35: infructescence shape, (0) globose, (1) compressed globose; character 40: peduncle L : W ratio, (0) less than 15 : 1, (1) 16–25 : 1, (2) >26 : 1, and character 46: seed coat anatomy, (0) mesotestal, (1) exotegmic. The current morphological matrix is presented in Table 4. Parsimony analysis was performed using a branch-and-bound search with MULPARS and furthest addition sequence options in PAUP* (version 4.0b10; Swofford, 2002). Character states were coded as unordered, and all characters were weighted equally. The amount of support for monophyletic groups revealed in the most parsimonious tree(s) (MPTs) was examined with 100 bootstrap replicates (Felsenstein, 1985) with the random addition and the heuristic search options.

Character diversification within Altingiaceae was investigated by comparing an analysis based on morphological data and molecular sequence data. We used sequences from our recently published combined analysis of five noncoding chloroplast regions (Ickert-Bond and Wen, 2006). We have excluded sampling of *Semiliquidambar* because of its putative hybrid origin, as suggested by several authors (Bogle, 1986; Ferguson, 1989; Ickert-Bond et al., 2005). Our molecular sampling in the current study is comparable to that used in the morphological data set (Table 2). Maximum parsimony was used to reconstruct phylogenetic relationships using heuristic search methods and addition sequence options as outlined in Ickert-Bond and Wen (2006). A strict consensus tree was generated, and the support of individual clades was estimated with the bootstrap method (Felsenstein, 1985). Bootstrap proportions (BP) were obtained from 2000 replicates of heuristic searches (1000 random addition sequences, tree-bisection-reconnection [TBR] branch swapping, and MulTrees selected).

RESULTS

Morphological description—general features of Altingia in comparison with Liquidambar (Figs. 1–25)—In contrast to *Liquidambar*'s typically spherical inflorescences, those of *Altingia* are spherical to occasionally elongate. Both develop into persistent, woody infructescences (Figs. 1, 3). They are composed of closely spaced, multiple (~6–35) bicarpellate fruits helically arranged around a central axis that extends into an elongate peduncle. Although infructescences are generally considered to be unisexual, it is not unusual to find a few, often presumably functional stamens, clustered within the infructescence heads in both genera (Fig. 6). While extrafloral structures of *Liquidambar* can be spine-like, those of *Altingia* are typically mammilate or knoblike (Fig. 11). Two species, *A. gracilipes* and *A. siamensis,* have a cuplike bract at the base of the infructescence (Figs. 3, 45, 65). Styles on inflorescences are short and recurved with broad stigmatic surfaces (Fig. 6). Stigmas are typically persistent in *Liquidambar* (Figs. 2, 7, 12) but are lacking in *Altingia*. However, style bases typically become sclerified, and these short, knob-like bases can occasionally be found on mature infructescences (Fig. 11). *Altingia* infructescences are similar to those of *L. acalycina* but differ from those of other species of *Liquidambar* in having a thicker and more differentiated fruit wall (Fig. 10) and more loosely attached fruits, with the infructescence disaggregating when sectioned (Figs. 8–9).

Bicarpellate fruits of Altingiaceae are fused basally and free distally (Figs. 13–20). Basally, the two locules are separate from one another (Figs. 19, 20), while more distally in the central part of the fruit the two carpels are open into a common locule (Figs. 17, 18). Dehiscence is a combination of septicidal and ventricidal (Figs. 14–16).

Individual carpels of *Altingia* are shorter and broader than those of most species of *Liquidambar*, except *L. acalycina* (Figs. 4, 5). Most *Altingia* species have a comparable fruit number to *Liquidambar* (25–40), but two species, *A. gracilipes*

Table 3. Extended.

Taxon	Carpel L (mm)	Carpel W (mm)	Carpel L : W	Carpel Ventr. wall surf.	Seed L (mm)	Seed W (mm)	Seed L : W	Seed coat
A. chinensis	6.73–9.23 ($\bar{X}$ = 7.88)	2.73–4.61 ($\bar{X}$ = 3.44)	2.00–2.86 : 1 ($\bar{X}$ = 2.32 : 1)	Single row, thick	4.43–5.67 ($\bar{X}$ = 5.16)	2.27–3.27 ($\bar{X}$ = 2.92)	1.45–2.26 ($\bar{X}$ = 1.77)	Polygonal
A. excelsa	5.26–6.83 ($\bar{X}$ = 6.26)	2.62–2.85 ($\bar{X}$ = 2.72)	2.62–2.85 : 1 ($\bar{X}$ = 2.30 : 1)	Single row, thick	4.38–6.12 ($\bar{X}$ = 5.24)	2.86–3.41 ($\bar{X}$ = 3.12)	1.51–1.85 ($\bar{X}$ = 1.67)	Polygonal
A. gracilipes	3.00–6.05 ($\bar{X}$ = 4.26)	1.67–3.14 ($\bar{X}$ = 2.28)	1.43–2.53 : 1 ($\bar{X}$ = 1.90 : 1)	Single row, thin?	7.15–10.49 ($\bar{X}$ = 8.94)	3.24–4.20 ($\bar{X}$ = 2.50)	2.49–2.75 ($\bar{X}$ = 2.50)	Polygonal
A. poilanei	5.04–8.42 ($\bar{X}$ = 6.76)	2.84–4.05 ($\bar{X}$ = 3.56)	1.42–2.26 : 1 ($\bar{X}$ = 1.91 : 1)	Single row, thick	7.15–10.49 ($\bar{X}$ = 9.34)	3.24–4.44 ($\bar{X}$ = 3.80)	2.05–2.75 ($\bar{X}$ = 2.47)	Polygonal
A. siamensis	4.04–6.75 ($\bar{X}$ = 5.37)	2.07–3.53 ($\bar{X}$ = 2.68)	1.58–2.56 : 1 ($\bar{X}$ = 2.02 : 1)	Multiple row, thick	5.62–7.44 ($\bar{X}$ = 6.78)	2.46–3.39 ($\bar{X}$ = 3.09)	1.94–2.58 ($\bar{X}$ = 2.21)	Polygonal

and *A. siamensis*, have only 6–9 fruits per infructescence (Fig. 3). Seeds of *Altingia* (and of *L. acalycina*) are ovoid with a circular flange (Fig. 4), in contrast to those of *L. formosana*, *L. orientalis,* and *L. styraciflua*, which are more ellipsoid and have a prominent distal wing (Fig. 5).

Fruits of *Altingia* and *Liquidambar* are anatomically similar, although there are several differences. The outer zone of the entire infructescence (of all the fruit walls collectively) is typically thicker and more highly differentiated in *Altingia* than in *Liquidambar*. While both genera have a region of tangentially elongate fibers in the outer fruit walls, this zone is more prominent in *Altingia* (Figs. 21, 22). To the periphery of this zone, the fruit walls in *Altingia* have several layers not typically present in *Liquidambar*. The first zone has numerous veins, which are each associated with resin canals and fiber bundles (Fig. 21). Next is a zone of cuboidal parenchyma cells about 8–10 cells thick, which are sparsely interspersed with resin canals. Within this region are shorter cells that appear to be tangentially divided and may have limited cambial activity (Fig. 21). To the outside is a region 3–4 cells thick of more elongate cells, typically filled with dark, tanniferous contents. The epidermis is uniseriate and is made up of palisade cells (Figs. 10, 21).

In contrast, the entire infructescence of *Liquidambar* is parenchymatous. Rather than producing a thick, compact infructescence with thickened peripheral fruit walls and only small remnants of style bases left behind as in *Altingia*, a larger proportion of tissue is committed to the extrafloral structures between adjacent fruits, which appear as elongate processes (Fig. 22). Only in the outermost boundary of the ground tissue are there regions with dark, tanniferous cells (Fig. 22). Differences are also evident within individual fruits; those of *Altingia* have more elaborate structure to the ventral margins where the carpels of each bicarpellate fruit are fused (Figs. 21, 23–25).

***Altingia chinensis* (Figs. 26–34)**—Infructescences are subglobose (Figs. 26, 28) and 18.04–24.94 ($\bar{X}$ = 21.79) mm high × 22.41–27.15 ($\bar{X}$ = 25.30) mm wide, with a length : width (L : W) ratio ranging from 0.75–1.00 : 1 ($\bar{X}$ = 0.86 : 1). Peduncles are 32.14–58.05 ($\bar{X}$ = 43.29) mm long × 1.32–2.30 ($\bar{X}$ = 1.69) mm wide (Fig. 26). Each inflorescence or infructescence is made up of 16–18 ($\bar{X}$ = 17.50) individual bicarpellate fruits (Figs. 26–29). Within mature inflorescences, styles are relatively short (up to 3 mm long), fairly thick, and strongly recurved (Fig. 27). Styles are deciduous and represented on mature infructescences only by slightly bumpy style bases where they were attached (Fig. 29). Individual fruits are 6.73–9.23 ($\bar{X}$ = 7.88) mm long × 2.73–4.61 ($\bar{X}$ = 3.44) mm wide (Fig. 29).

The fruit wall is two-parted (Fig. 31). It is composed of an outer region ~25–30 cells thick (Figs. 31, 33) and an inner, uniseriate palisade layer of macrosclereids (Figs. 30, 32). Individual rectangular cells of the palisade layer are vertically elongate and have somewhat unevenly thickened cell walls (Fig. 30). The outer fruit wall is parenchymatous with cells that are isodiametric to slightly elongated tangentially and appearing stretched, vascular bundles with prominent fibers and

Table 4. Data matrix for morphological analysis of Altingiaceae and close relatives.

Taxon (Character numbers)	1	2	3	4	5	6	7	8	9	10	11	12	13	14	15	16	17	18	19	20	21	22	23	24	25	26	27	28	29	30	31	32	33	34	35	36	37	38	39	40	41	42	43	44	45	46	47	48	49
Hamamelis virginiana	0	0	0	0	0	?	0	0	0	0	0	0	0	0	0	0	1	0	0	0	0	0	0	0	0	?	?	1	?	1	0	0	0	1	?	0	1	0	0	0	0	0	0	0	0	0	?	0	0
Exbucklandia populnea	0	1	1	1	2	?	0	?	1	0	0	0	0	0	0	0	1	0	0	0	1	0	0	0	0	?	?	?	?	?	1	1	0	1	?	1	1	0	0	0	0	0	0	0	1	0	?	0	2
Microaltingia apocarpela	?	?	?	?	?	?	0	?	0	?	?	?	?	?	?	0	0	0	0	1	1	?	0	?	?	0	?	?	?	0	2	?	1	0	0	1	?	?	0	0	?	?	0	?	?	?	?	?	?
Liquidambar changii	?	?	?	?	?	?	?	?	1	1	?	?	?	?	?	?	?	?	?	1	0	1	0	0	0	0	0	0	0	1	2	1	1	2	0	2	0	?	1	2	1	0	2	1	1	1	0	?	?
Altingia chinensis	1	0	0	0	1	0	1	1	1	1	1	0	1	0	1	1	0	1	1	1	1	0	0	1	0	1	0	1	0	1	2	1	2	2	0	2	1	1	1	2	0	0	2	1	1	1	0	1	1
A. excelsa	0	0	0	0	1	0	1	1	1	1	1	0	1	0	1	1	0	1	1	1	1	0	0	1	0	1	0	1	0	1	2	1	2	1	1	2	1	1	1	1	0	0	2	1	1	1	0	1	1
A. poilanei	1	0	0	0	1	0	1	1	1	1	1	0	1	0	1	1	0	1	1	1	1	0	0	1	0	1	0	1	0	1	2	1	2	2	3	2	1	1	1	0	0	0	2	1	1	1	0	1	1
A. gracilipes	1	0	0	0	1	0	1	1	1	1	1	0	1	0	1	1	0	1	1	1	1	0	0	1	0	1	0	0	0	?	2	1	2	1	2	1	1	1	1	1	0	0	2	1	1	1	0	1	1
A. siamensis	0	0	0	0	1	0	1	1	1	1	1	0	1	0	1	1	0	1	1	1	1	0	0	1	0	1	1	1	0	0	2	1	2	1	2	1	1	1	1	1	0	0	2	1	1	1	0	1	1
L. acalycina	0	1	1	1	2	0	1	1	1	2	1	1	0	1	1	1	0	1	1	1	0	1	0	0	1	0	0	0	0	0	2	1	1	2	0	2	0	1	1	2	1	0	2	1	1	1	0	1	1
L. formosana	0	1	1	1	2	0	1	1	1	2	1	1	0	1	1	1	0	1	1	2	0	1	1	0	1	0	0	0	1	1	2	1	1	2	0	2	0	1	1	2	1	1	1	1	1	1	1	1	1
L. orientalis	0	1	1	1	2	1	1	1	1	1	1	1	0	1	1	1	0	1	1	2	0	1	0	1	1	0	0	1	1	1	2	1	1	1	0	3	0	1	1	1	1	1	1	1	1	1	1	1	1
L. styraciflua	0	1	1	1	2	1	1	1	1	1	1	1	0	1	1	1	0	1	1	2	0	1	0	1	1	0	0	1	1	1	2	1	1	2	0	2	0	1	1	2	1	1	1	1	1	1	1	1	1

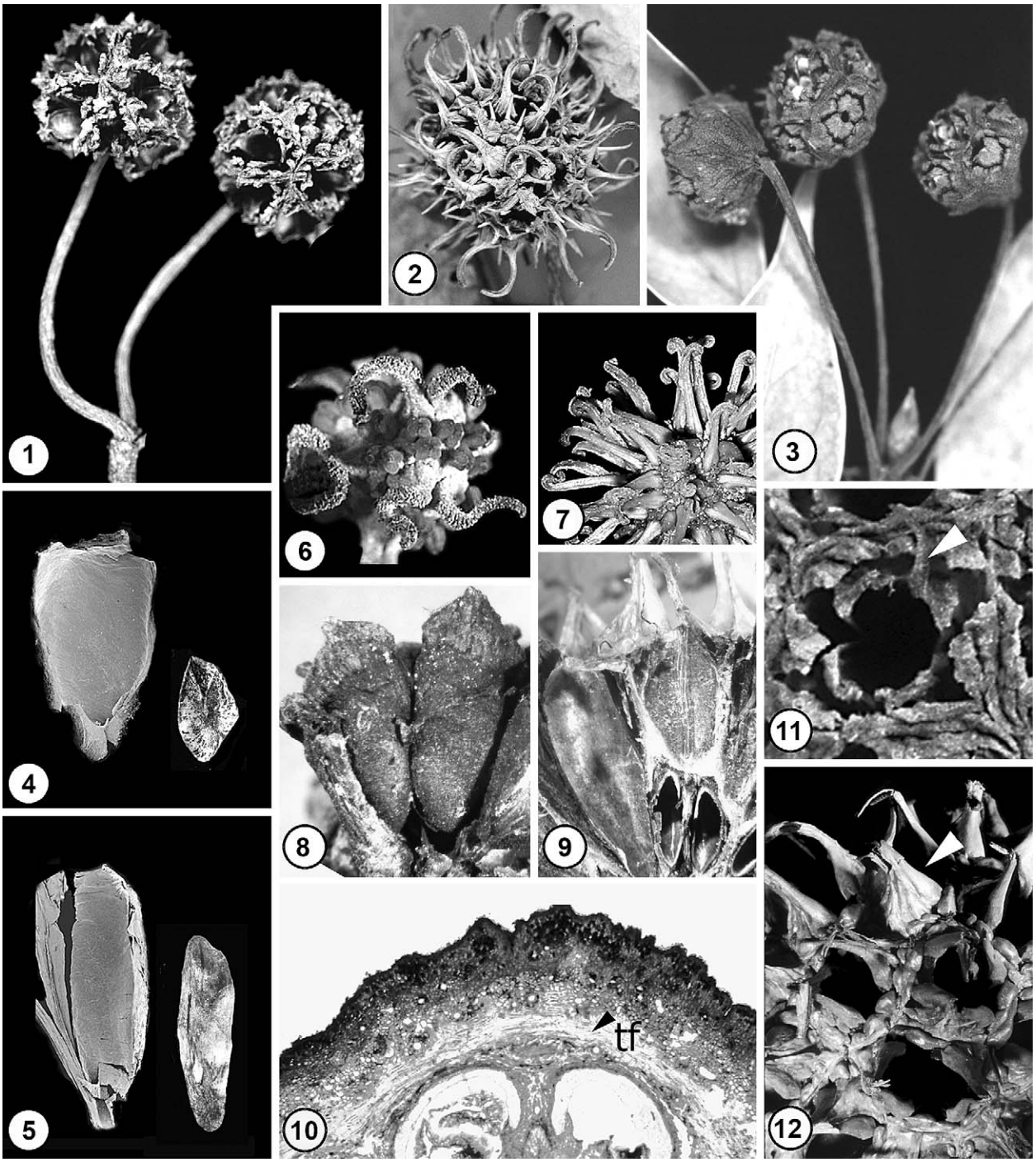

Figs. 1–12. General features of infructescences and inflorescences of *Altingia* (Figs. 1, 3–4, 6, 8, 10, 11) and *Liquidambar (*Figs. 2, 5, 7, 9, 12). **1.** Two mature globose, long pedunculate infructescences of *A. excelsa*, ×1.1. **2.** Infructescence of *L. acalycina*, showing paired, recurved styles and prominent spines, ×1.5. **3.** Infructescence of *A. gracilipes* with basally attached peduncles. Note cuplike bracts surrounding fruits (at left), ×2.4. **4.** SEM of longitudinal hand-section of *A. poilanei* carpel revealing broad shape and seed with encircling flange (at right), ×4.2. **5.** SEM of longitudinal hand-section (LHS) of *L. formosana* carpel revealing narrow, elongate shape and seed with distal wing (at right), ×4.7. **6.** Inflorescence in *A. siamensis* showing large, recurved styles with broad stigmatic surfaces on short style bases. Note stamens in center of inflorescence with sessile anthers, ×3.8. **7.** Inflorescence in *L. styraciflua* showing large, recurved styles with broad stigmatic surfaces on long style bases. Note stamens in center of inflorescence with sessile anthers, ×3.0. **8.** LHS of *A. siamensis* revealing loosely attached bilocular fruits, ×3.9. **9.** LHS of *L. styraciflua* to show tight connection between adjacent bilocular fruits, ×3.0. **10.** Transverse section of Paraplast-embedded infructescence of *A. gracilipes* showing organization of outer infructescence with prominent tangential fiber zone (tf) at arrow, ×11.4. **11.** Detail of mature infructescence of *A. chinensis* showing mammilate extrafloral structures. Note persistent style base (arrow), ×2.2. **12**. Detail of mature infructescence of *L. styraciflua* with exserted fruits (arrow). Note bumpy, "braided" appearance of extrafloral structures, ×3.1.

separate fiber bundles, and numerous, well-defined resin canals up to 8 μm in diameter (Fig. 34). Fiber bundles, as seen in transverse section, are rectangular and tangentially elongate, ~10 cells thick × 30 cells wide. Seeds are 4.43–5.67 ($\bar{X} = 5.16$) mm long × 2.27–3.27 ($\bar{X} = 2.92$) mm wide (L : W ratio = 1.77 : 1) with a circular flange surrounding the central body.

Distinctive features of this species include medium-sized infructescences containing numerous fruits ($\bar{X} = 15$) borne on very long and thick peduncles, a sclerenchymatous, uniseriate, palisade inner fruit wall with relatively elongate cells, and relatively short, thick, and strongly recurved styles in pistillate flowers.

Altingia excelsa (Figs. 35–44)—Infructescences are compressed-globose and 13.94–16.55 ($\bar{X} = 15.73$) mm high × 15.65–22.22 ($\bar{X} = 19.03$) mm wide with a length : width (L : W) ratio ranging from 0.65–1.02 : 1 ($\bar{X} = 0.84 : 1$) (Fig. 35, 37–38). Peduncles are 22.05–38.47 ($\bar{X} = 29.35$) mm long × 0.75–1.70 ($\bar{X} = 1.36$) mm wide. Each inflorescence or infructescence is made up of ~9–25 ($\bar{X} = 15$) individual bicarpellate fruits. Pistillate flowers have straight, thick styles, and the entire infructescence is subtended by hyaline bracts (Fig. 36). Remnants of the style bases are still present on many fruits (Fig. 37).

The fruit wall is composed of a uniseriate, sclerenchymatous, inner palisade layer (Fig. 41) and an outer region 15 cells thick (Fig. 39). Cells of the palisade layer are only slightly vertically elongate, almost cuboidal in shape with highly unevenly thickened walls (Fig. 41). The outer fruit tissue has a thick, tangentially elongate layer; a fairly large zone of fibers with interspersed resin canals (Figs. 42, 43); and vascular tissue including vessel elements with oblique perforation plates (Fig. 44). Seeds (Fig. 40) are 4.80–6.12 ($\bar{X} = 5.53$) mm long × 2.86–3.31 ($\bar{X} = 3.19$) mm wide (L : W ratio = 1.73 : 1).

Distinctive features of this species include compressed globose infructescences borne on relatively long and thin peduncles; a uniseriate, palisade inner fruit wall with almost cuboidal cell shape and highly unevenly, thickened walls; as well as a medium number of fruits ($\bar{X} = 15$) per infructescence. Pistillate flowers have almost straight styles, and the inflorescences are subtended by hyaline bracts.

Altingia gracilipes (Figs. 45–54)—Infructescences are obconical and 9.56–13.44 ($\bar{X} = 11.96$) mm high × 11.86–16.90 ($\bar{X} = 14.67$) mm wide with a length : width (L : W) ratio ranging from 0.74–0.91 : 1 ($\bar{X} = 0.82 : 1$) (Figs. 45, 46). Peduncles are 14.93–28.18 ($\bar{X} = 22.26$) mm long × 0.85–1.24 ($\bar{X} = 1.04$) mm wide (Fig. 45). Each inflorescence or infructescence is made up of ~5–6 ($\bar{X} = 5.78$) individual bicarpellate fruits (Figs. 48, 49). A distinctive, cuplike bract subtends each infructescence (Fig. 45). Style bases appear as small, beaklike structures on slightly raised circular platforms (Fig. 46).

Fruits are 7.15 mm long × 3.48 mm wide and elongate (Fig. 47). The fruit wall is composed of an inner sclerenchymatous palisade layer 1–2 cells thick (Figs. 50, 53, 54) and a three-zoned outer region (Figs. 48, 52). Cells of the palisade layer are vertically elongate and 5–6 sided. Where the ventral margins of the adjacent carpels of the fruit meet, the region of the fruit wall immediately to the outside of the palisade layer is composed of a dark, fibrous tissue. This darker tissue extends around and encircles the palisade layer as extensions of the septum (Figs. 50, 53). The outer fruit wall contains an inner zone with small vascular bundles that are associated with small fiber bundles and abundant resin canals (Figs. 50, 53). This zone is surrounded by tangentially elongate, fibrous cells that encircle the inner area of the fruit (Fig. 48, 52). The outer fruit wall is composed of numerous, larger vascular bundles, fiber bundles, resin canals, and 4–5 rows of slightly radially elongate cells with dark contents. (Figs. 51, 52). The epidermis is uniseriate. Seeds are 3.00–6.05 ($\bar{X} = 4.26$) mm long × 1.67–3.08 ($\bar{X} = 2.28$) mm wide (L : W ratio = 1.90 : 1) and have a light brown halo at the edge of the circular flange that surrounds the central seed body.

Distinctive features of this species include the leafy cuplike bract subtending each infructescence (Fig. 45), obconical infructescence shape, small number of bicarpellate fruits, and well-differentiated outer fruit wall (Figs. 48, 52).

Altingia poilanei (Figs. 55–64)—Infructescences are turbinate (Figs. 55, 56) and 21.91–30.98 ($\bar{X} = 26.94$) mm high × 21.47–26.80 ($\bar{X} = 23.87$) mm wide, with a length : width (L : W) ratio ranging from 0.59–0.79:1 ($\bar{X} = 1.124 : 1$). Peduncles are 20.26–31.49 ($\bar{X} = 24.23$) mm long × 0.93–1.20 : 1 ($\bar{X} = 1.08$) mm wide. Each infructescence is generally made up of ~25 individual bicarpellate fruits (Figs. 56, 59, 60), although triloculate carpels were also observed (Fig. 57).

The fruit wall is composed of an inner palisade layer of sclereids 1–2 cells thick (Figs. 61, 62) and an outer fruit wall (Figs. 58, 63). Cells of the palisade layer are thick-walled and vertically elongate and variably 4–5 sided. Fibers with large lumina are associated with the region of ventral carpel fusion in the fruit tissue (Fig. 64). Resin canals associated with fiber bundles are dispersed evenly throughout the outer fruit wall. Lenticel-like structures (Fig. 63) occur on the surfaces of the fruits. Seeds are 5.04–7.61 ($\bar{X} = 6.50$) mm long × 2.84–4.05 ($\bar{X} = 3.53$) mm wide (L : W ratio = 1.86 : 1).

Distinctive features of this species include turbinate infructescence shape, large size, numerous fruits per infructescence ($\bar{X} = 25$), fibers with large lumina in the fruit tissue, and a lobed outer fruit wall with lenticel-like structures in the epidermis.

Altingia siamensis (Figs. 65–75)—Infructescences are compressed globose and 8.70–13.48 ($\bar{X} = 11.27$) mm high × 11.70–21.65 ($\bar{X} = 15.81$) mm wide, with a length : width (L : W) ratio ranging from 0.59–0.79 : 1 ($\bar{X} = 0.71 : 1$) (Figs. 65, 66). Peduncles are 20.26–31.49 ($\bar{X} = 24.23$) mm long × 0.93–1.20 ($\bar{X} = 1.08$) mm wide (Fig. 65). Each inflorescence or infructescence is made up of ~6–7 individual bicarpellate fruits (Figs. 66–68, 71). A cuplike bract, similar to that of *A. gracilipes* but less well developed, subtends each infructescence (Fig. 65). Carpels bear short, stout, recurved styles with broad, elongate stigmatic areas (Fig. 69, 70).

The carpel wall is composed of an inner sclerenchymatous palisade layer one-to-several cells thick and an outer fruit wall that appears relatively thin compared to that of other *Altingia* species (Fig. 72). Resin canals, somewhat flattened tangentially, are associated with distinctive arclike fiber bundles (Figs. 72, 73, 75). Both resin canals and arclike fiber bundles are more pronounced in the outer fruit wall. The palisade layer is composed of very thin, vertically elongate sclerenchymatous cells with uniformly thin walls (Fig. 74). Seeds are 4.04–6.75 ($\bar{X} = 5.37$) mm long × 2.0.7–3.53 ($\bar{X} = 2.68$) mm wide (L : W ratio = 2.00 : 1).

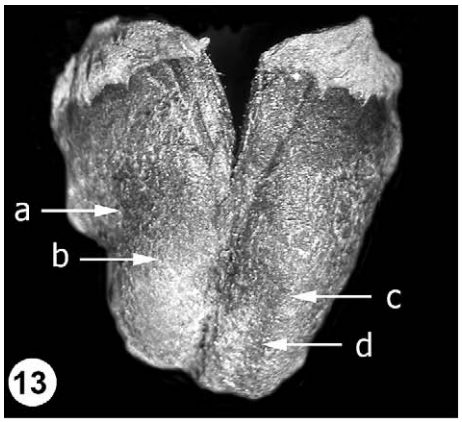
a
b
c
d
13

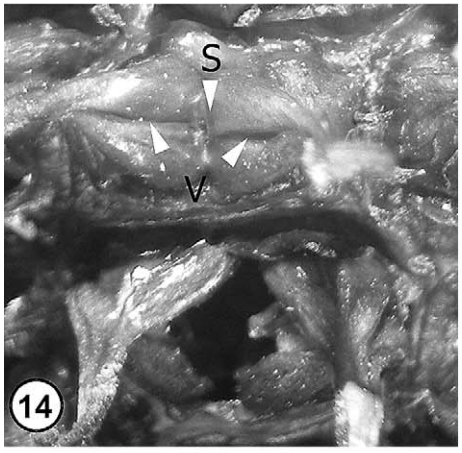
S
V
14

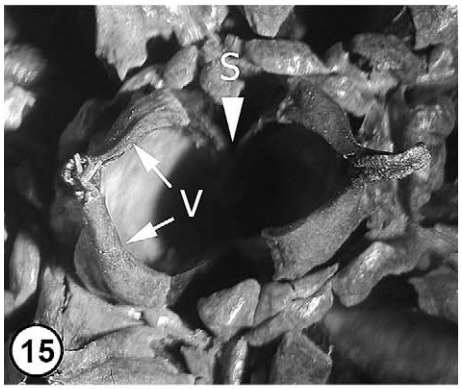
S
V
15

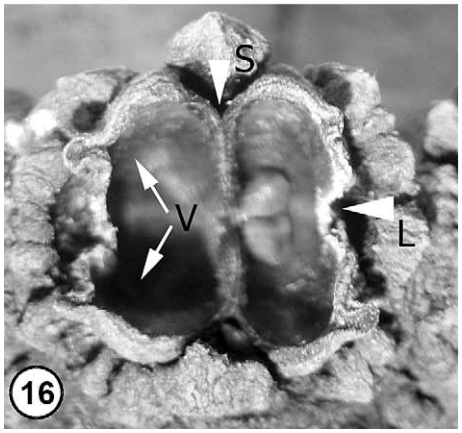
S
V
L
16

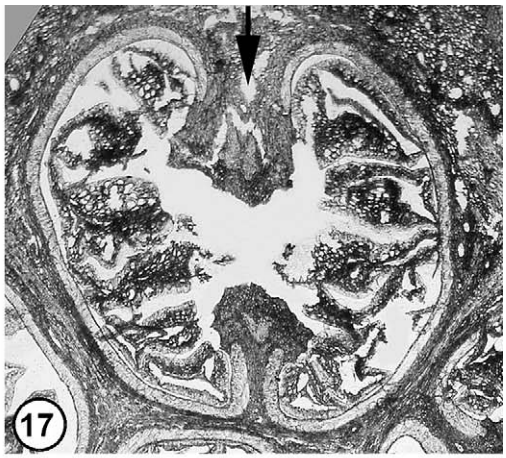
17

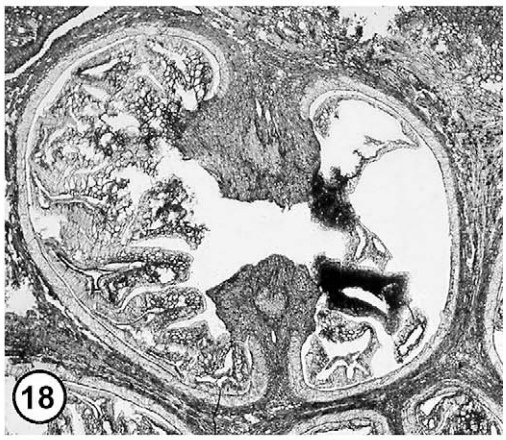
18

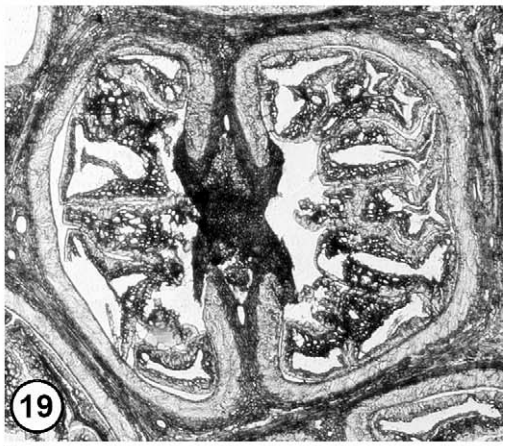
19


20

Distinctive features of this species include small, compressed, globose infructescences subtended by a cuplike bract (Fig. 65), few fruits per infructescence ($\bar{X} = 6$), and numerous resin canals throughout the outer fruit tissues, each associated with an arclike fiber bundle cap (Figs. 72, 73).

Seed morphology and anatomy (Figs. 76–85)—While a large number of anatropous ovules are borne on the ventral margin of each carpel in *Altingia*, only a few typically mature into seeds. As in *Liquidambar*, viable seeds tend to be produced near the infructescence axis. Mature seeds in *Altingia* are broadly ovate with a circular flange (Figs. 76, 78) and 5–9 mm long × 2.5–4 mm wide (Table 3). They are typically speckled or striped, but none of this variation is species specific (Fig. 4). Seed surface micromorphology is fairly homogenous. Cells are arranged parallel to the long axis of the seed and are more or less polygonal (Figs. 79–81). The seed coat has five tissue layers based on differing cell types (Figs. 82–85), with the outermost layer a uniseriate epidermis (Fig. 83, 85). Beneath the epidermis is a hypodermal zone 1–2 cells thick of parenchyma containing calcium oxalate crystals (Figs. 83, 85), followed by a third layer 2–3 cells thick of thin, tangentially elongate, crushed parenchyma (Fig. 84). To the inside is a fourth zone 2–3 cells thick, which is the mechanical layer and is composed of macrosclereids (Figs. 84, 85). To the inside of this layer is a fifth zone of often crushed, tangentially elongate cells 1–2 cells thick that may represent the nucellus (Fig. 84).

Phylogenetic analysis based on morphological data—The phylogenetic analysis of the Altingiaceae and its close extant and fossil relatives, with *Exbucklandia* and *Hamamelis* as outgroups, revealed a single MPT of 78 steps with a consistency index (CI) of 0.79 and a retention index (RI) of 0.86 (Fig. 86). Of 49 character state changes, 42 were parsimony informative. The family Altingiaceae is monophyletic with the Cretaceous fossil from eastern North America, *Microaltingia apocarpela* sister to the clade of extant Altingiaceae. *Microaltingia* has several characters that are consistent with those of extant Altingiaceae. However, the pollen and seed morphology of this genus differs from the family. *Altingia* is strongly supported as sister to *Liquidambar* (BP = 96%). Within *Liquidambar*, the Middle Miocene fossil *L. changii* is basal, sister to a clade of extant *L. acalycina* and a clade of *L. formosana*, which is sister to the subclade of *L. styraciflua* and *L. orientalis* (Fig. 86). Within *Altingia,* relationships are less well resolved, and *A. chinensis* and *A. poilanei* form a clade that is sister to a clade of *A. excelsa* and a subclade of *A. siamensis* and *A. gracilipes* (Fig. 86).

Morphological characters have also been examined according to their distribution on the tree. Thirty-six of the 49 characters are not homoplasious (CI = 1.0), while the remaining 13 have different levels of homoplasies. One character (character 28: inner carpel wall anatomy) is highly homoplasious with a CI of 0.33. This character reverses two times on the phylogeny and diverges once (Fig. 86). Two of the homoplasious characters have convergences (characters 1 and 24), while 11 have both convergences and reversals (characters 2, 3, 4, 5, 9, 10, 21, 28, 34, 37, 40).

Phylogenetic analysis based on molecular data—Analysis of the combined cpDNA data revealed three MPTs of 719 steps with a CI = 0.98 and a RI = 0.92. The strict consensus tree when rooted with *Hamamelis virginiana* shows a strongly supported monophyletic Altingiaceae (Fig. 87; BP = 100%). Furthermore, three distinct clades are highly supported: (1) a *L. styraciflua* and *L. orientalis* clade (BP = 100 %); (2) a clade of two species from China and North Vietnam, *A. chinensis* and *A. poilanei* (BP = 97 %); and (3) a clade containing the remaining taxa. Within this larger well-supported clade (BP = 91%), a clade of *A. excelsa* from Indonesia to southern China and *A. siamensis* from Indochina diverges at the base, sister to a highly supported clade (BP = 96%) composed of *A. gracilipes*, *L. formosana*, and *L. acalycina*.

DISCUSSION

Infrageneric variation in Altingia—Species of *Altingia* are all of similar morphologic construction. The major distinguishing characters are infructescence size, shape and fruit number. Another distinctive feature is the presence or absence of a cuplike bract subtending the infructescence and its size. Hyaline bracts also occur at least in some species but are only rarely found, probably because of their ephemeral nature and early deciduousness. Other characters that are variable and of potential taxonomic value include: structure of ventral carpel walls in fruits, details of outer fruit wall, distribution and shape of fiber bundles, and number and distribution of resin canals.

Infructescence size and shape, fruit number, and details of axis in Altingia—The number of fruits per infructescence is correlated with the size of the infructescence and equates to roughly one fruit per millimeter of axis length. The largest infructescence (*A. poilanei*, $\bar{X} = 27$ mm long) also has the largest number of fruits ($\bar{X} = 25$), those of intermediate size have fewer fruits (*A. chinensis*, $\bar{X} = 18$ mm, $\bar{X} = 18$ fruits; *A. excelsa*, $\bar{X} = 16$ mm, $\bar{X} = 15$ fruits), and the smallest infructescences *A. gracilipes* ($\bar{X} = 11$ mm) and *A. siamensis* (12 mm) have very few fruits (six each) (Table 3) (Ferguson, 2002). The shape of infructescences in *Altingia* ranges from globose (*A. chinensis*), to obconical (*A. gracilipes* and *A. siamensis*), to slightly elongate to turbinate (*A. poilanei)*. The

←

Figs. 13–20. Details of fruit structure and dehiscence of *Altingia siamensis* (Figs. 13, 16), *Liquidambar styraciflua* (Figs. 14, 15), *A. gracilipes* (Figs. 17–19), and *A. poilanei* (Fig. 20). **13.** Dissected fruit showing fused basal and free distal carpels. Levels indicate relative positions of sections seen in Figs. 17–20. a, Fig. 17; b, Fig. 18; c, Fig. 19; d, Fig. 20; ×5.8. **14.** Two *Liquidambar* biloculate fruits, top view. Top fruit shows fused ventral margins of carpels, prior to dehiscence. Septicidal (S) and ventricidal (V) lines of dehiscence are indicated. Bottom fruit shows primarily S and beginning of V dehiscence (at right), ×8.2. **15.** *Liquidambar* biloculate fruit, top view showing S and V dehiscence, in slightly older fruit, ×8.51. **16.** *Altingia* biloculate fruit, top view, showing S and V dehiscence, as in *Liquidambar*. Additionally, loculicidal dehiscence (L) occurs at the outer dorsal margin, ×6.2. **17.** Distalmost level (= Fig. 13d), showing carpels slightly below the free-carpel level. Note split on top, indicating S dehiscence (at arrow), ×12.7. **18.** More proximal level (= Fig. 13c) showing common locule between the two fruits, ×13.8. **19.** Central level (= Fig. 13b) showing fused ventral margins with elaborated features, ×15.8. **20.** Basalmost level (= Fig. 13a) showing carpels with ventrally fused margins making up central septum, ×16.2.

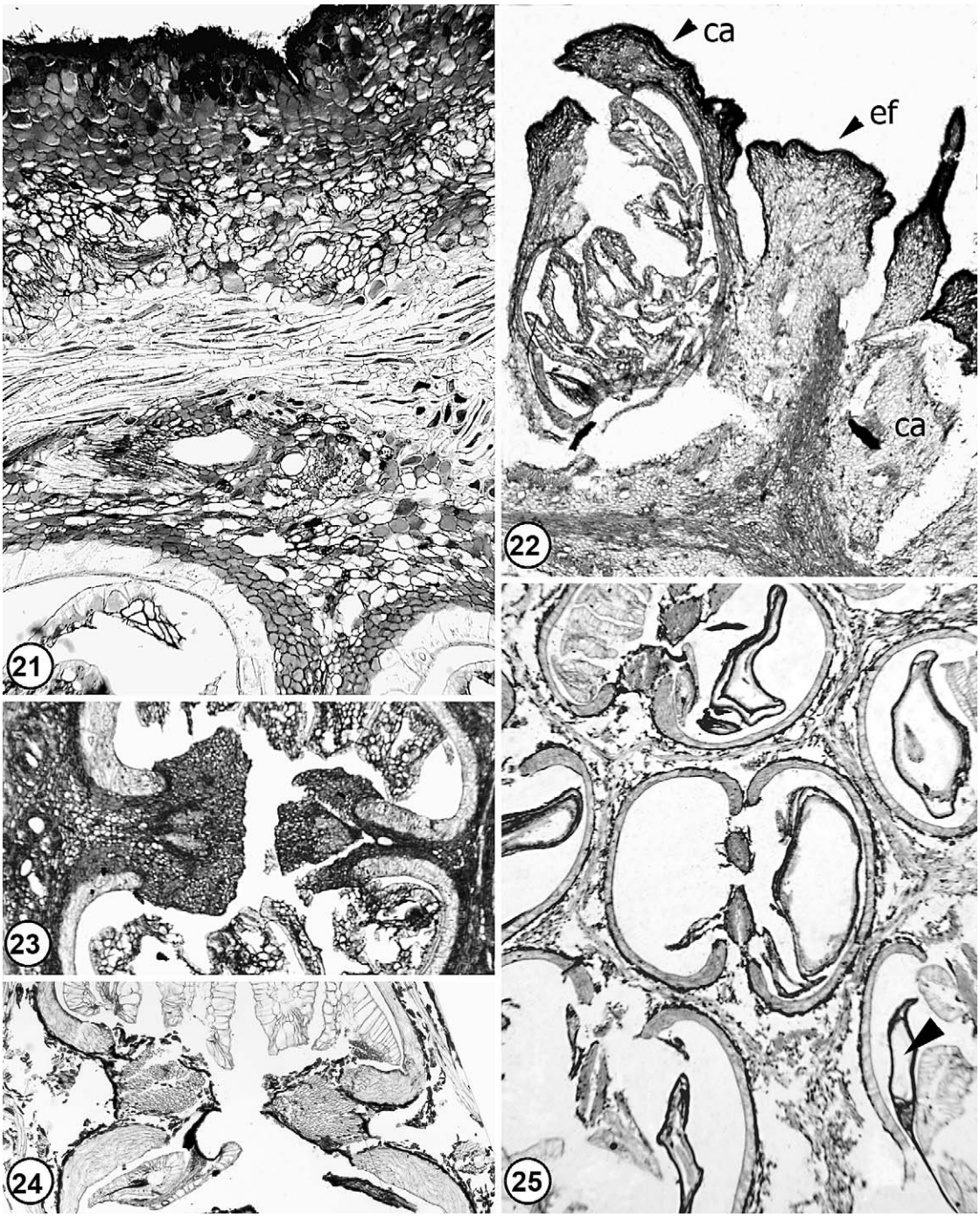

Figs. 21–25. Anatomical features of *Altingia* (Figs. 21, 23) and *Liquidambar* (Figs. 22, 24, 25) infructescences in transverse sections. **21.** Paraplast-embedded infructescence of *A. gracilipes* showing organization of outer fruit wall, ×27.3. **22.** Paraplast-embedded infructescence of *L. orientalis* showing organization of outer fruit wall. Note dark zone of horizontally oriented fibers in outer wall. Note extrafloral processes (ef) between adjacent carpels (ca), ×15.0. **23.** *A. gracilipes* fruit at proximal level showing ventral fusion of two adjacent carpels in bicarpellate fruit. Note that "pads" of fused tissues of adjacent carpels are extensively flanged, ×23.5. **24.** *L. acalycina* fruit at proximal level showing ventral fusion of two adjacent carpels in bicarpellate fruit. Note less prominent "pads" of fused tissues, ×21.8. **25.** *L. formosana* showing bicarpellate fruits. Note seed with distal wing at arrow, ×15.8.

infructescences of both *A. gracilipes*, and to a lesser extent *A. siamensis*, are subtended by a cuplike bract (Figs. 3, 45, 65).

Peduncle length varies from very long in *A. chinensis* (43 mm) to long in *A. excelsa* (29 mm), while the shortest are in *A. poilanei, A. siamensis* (both 24 mm), and *A. gracilipes* (22 mm). Peduncle width is not consistently correlated with length, as previously noted by Ferguson (1989). While *A. chinensis*, which has the longest peduncles (43 mm), also has one of the thickest (1.7 mm wide); the relatively short peduncles of *A. poilanei* (24 mm) are also thick (1.8 mm). The shortest

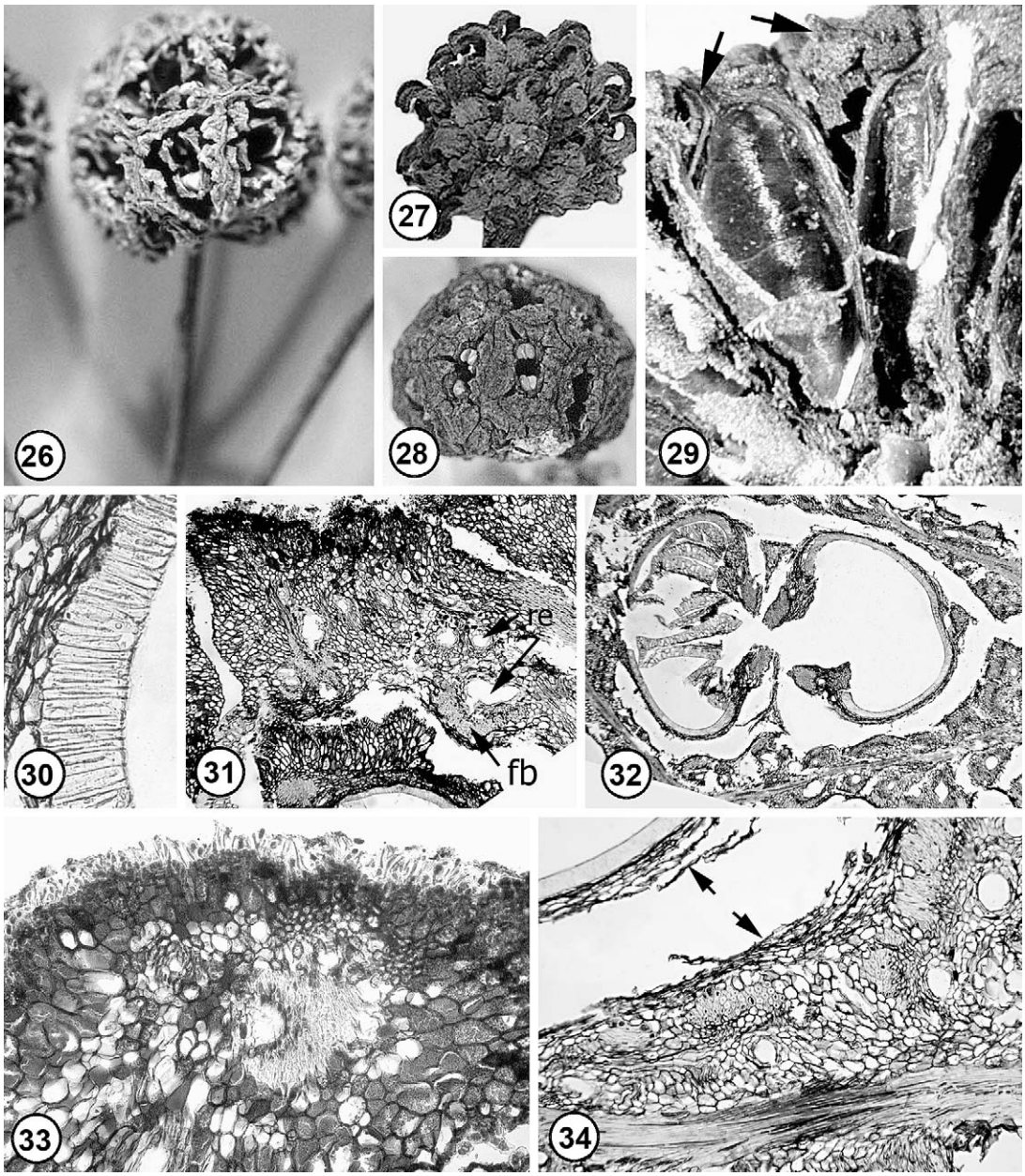

Figs. 26–34. *Altingia chinensis* infructescences and inflorescences. **26.** Mature infructescence on elongate peduncle, ×1.4. **27.** Inflorescence showing short, highly recurved styles with expanded stigmatic areas, ×1.8. **28.** Mature infructescence showing broad mammilate tubercles between adjacent fruits, ×1.4. **29.** Longitudinal handsection of infructescence. Note shiny, thickened inner carpel wall and persistent style bases (at arrows), ×5.8. **30.** Inner carpel wall structure, showing single-cell layer of macrosclereids on surface, and underlying parenchyma tissue, ×39.6. **31.** Outer fruit wall tissue showing vascular bundles with associated resin canals (re) and fiber bundles (fb), ×10.2. **32.** Cross section of bicarpellate fruit showing separation of inner carpel wall and outer fruit tissue along plane of weakness close to carpel wall. Note aborted seeds (at left), ×7.3. **33.** Detail of outer fruit wall, with epidermal cells at top, ×19.3. **34.** Detail of tissues in Fig. 32, lower right. Note separation along plane of weakness within infructescence near inner carpel wall (arrows). Note tangentially elongated fibers encircling individual fruits at bottom, ×43.9.

peduncles, on *A. siamensis* (24 mm long) and *A. gracilipes* (22 mm long), are also the thinnest (1.1 mm and 1.0 mm wide, respectively).

Infructescence anatomy in Altingia—Additional differences between species of *Altingia* are based on variation in the anatomy of the infructescence ground tissue, including details of inner carpel wall and outer fruit tissues. Inner palisade carpel walls of most species of *Altingia* are uniseriate, but in *A. siamensis* this region may be up to four cells thick (Fig. 74). The palisade cells of the inner carpel wall vary among the taxa in shape and wall thickness from cuboidal and thick walled (*A. excelsa*), to somewhat radially elongate and thick walled (*A. chinensis*, *A. gracilipes*, *A. poilanei*), to elongate with quite thin walls (*A. siamensis*). Wall thickness can also vary within a cell.

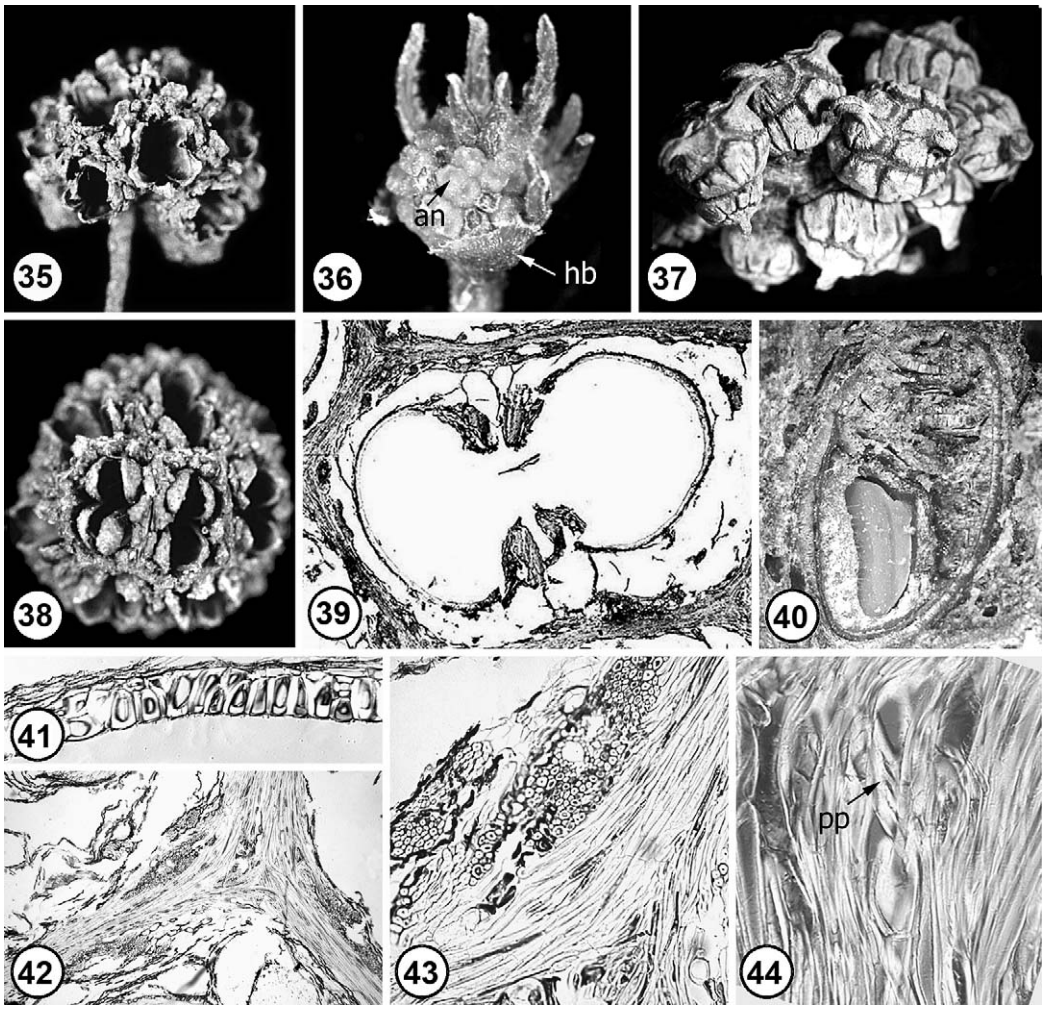

Figs. 35–44. *Altingia excelsa* infructescences and inflorescences. **35.** Weathered infructescence, ×1.8. **36.** Inflorescence with long, almost straight styles. Note interspersed anthers (an) and subtending hyaline bract (hb), ×4.6. **37.** Detail of individual fruits prior to dehiscence. Note small, persistent style bases, ×3.1. **38.** Detail of mature infructescence showing mammilate tubercles between adjacent fruits. Note absence of persistent style bases, ×1.9. **39.** Cross section of bicarpellate fruit showing separation of inner carpel wall and outer fruit tissue along plane of weakness, ×7.4. **40.** Detail of fruit in longitudinal section, showing maturing embryo in seed and aborted ovules above, ×6.9. **41.** Detail of uniseriate epidermis of macrosclereids forming the surface of the inner carpel wall, ×22.9. **42.** Tangentially elongate fibers in outer fruit walls, ×6.7. **43.** Detail of outer fruit wall showing fiber bundles, resin canals, and tangentially elongate fibers, ×18.2. **44.** Detail of vascular tissues showing vessel elements with oblique perforation plates (pp) at arrow, ×53.4.

In the outer fruit wall, the distribution and shape of fiber bundles and resin canals can vary. All species contain these elements, but resin canals are considerably larger and more numerous in the outer fruit walls in *A. siamensis* than in other species (Figs. 72, 73). In addition, the resin canals of *A. siamensis* are associated with arclike fiber bundles (Fig. 73), whereas other species have less well-defined bundles with fewer fibers. Fruits all have outer fruit walls with tangential fiber zones, but this feature is particularly well developed in *A. gracilipes* (Figs. 10, 52). All fruits have a uniseriate epidermis; however, in *A. poilanei* the outermost fruit wall has lenticel-like structures that presumably develop from periclinal divisions of the outer ground tissue (Fig. 63).

Infrafamiliar variation: fruit dehiscence in Altingiaceae—An important taxonomic character that has been used to separate genera within Altingiaceae is variation in dehiscence type (Ferguson, 1989; Zhang et al., 2003). However, two problems have been inherent in using dehiscence as a taxonomic character: (1) differences in terminology used (Table 5), and (2) problems in understanding the process.

One basic problem with terminology is that different terms have been used for the same structures by various authors. In *Altingia*, dehiscence has been reported by many to be loculicidal and septicidal, resulting in four separate valves (Mai, 1968), while *Liquidambar* and *Semiliquidambar* are described as septicidal (Table 5) (Ferguson, 1989). These authors are identifying the septum of septicidal dehiscence as the area created by the fused ventral margins of the two carpels that make up the bicarpellate fruit. Loculicidal in this case refers to the splitting of each carpel at right angles to the septum (in the center). In contrast, Endress (1989a) described dehiscence in *Liquidambar* as septicidal and ventricidal. Endress thus uses the term septicidal in the same sense as the previous authors but refers to the separation of the ventral margins of each individual fruit as ventricidal rather than

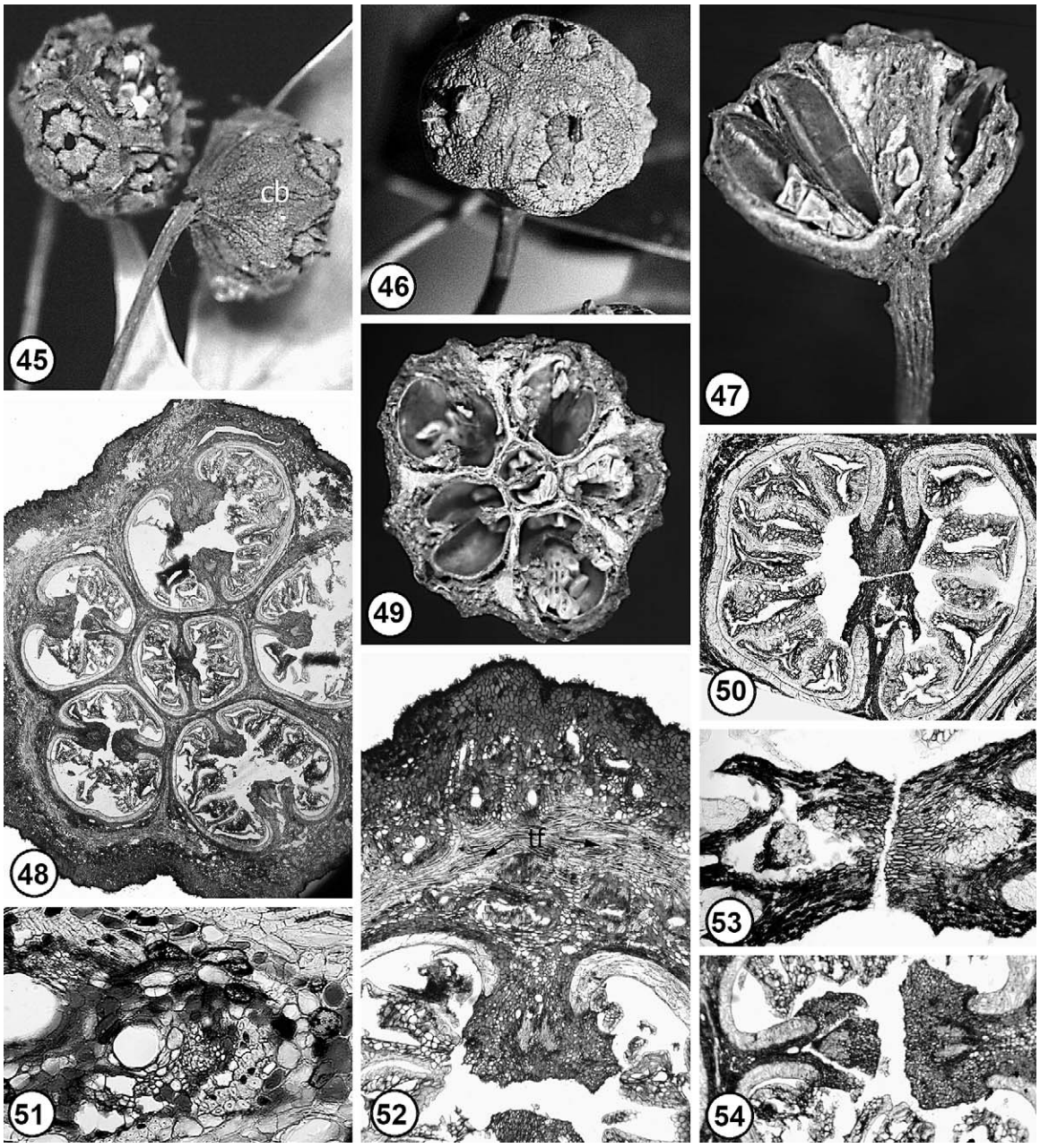

Figs. 45–54. *Altingia gracilipes* infructescences and inflorescences. **45.** Infructescence with basal attachment of peduncle. Note cuplike bracts surrounding fruits (cb), ×2.2. **46.** Mature infructescence prior to dehiscence. Note small, persistent style bases and small, mammilate tubercles between and surrounding adjacent fruits, ×2.3. **47.** Longitudinal hand-section of infructescence, ×2.4. **48.** Transverse section (TS) of Paraplast-embedded infructescence showing several fruits at different levels, ×4.8. **49.** Transverse hand-section of infructescence revealing several bicarpellate fruits, ×3.3. **50.** TS of individual fruit, ×14.7. **51.** Detail of inner region of fruit wall showing vascular bundles with associated resin canals and fiber bundles, ×20.7. **52.** TS of infructescence, showing adjacent carpels of one fruit (at bottom) and zonation of outer infructescence wall (at top). Note tangential fiber zone (tf) at arrows, ×23.9. **53.** Detail of ventral margins of carpels within an individual fruit showing septicidal dehiscence, ×22.3. **54.** Section similar to Fig. 53, showing septicidal dehiscence and beginning of ventricidal (at left), ×18.1.

loculicidal. However, Endress follows Mai (1968) in suggesting that *Altingia* and the fossil *Steinhauera* dehisce septicidally and loculicidally. Zhang et al. (2003) use loculidicidal for *Altingia* and *Liquidambar* and also describe the resulting structure (Table 5).

To clear up this confusion, we look to the original definition of the terms. Winkler (1936) defined dehiscence as septicidal if it occurs longitudinally along the juncture of adjacent carpels or loculicidal if it occurs along the plane of the median (central or dorsal) bundle of each carpel (Stopp, 1950; Esau, 1965). Ventricidal dehiscence occurs along the inner or ventral surfaces of a carpel, where its adjacent lateral arms meet (Stopp, 1950). In this sense, we concur with Endress's use of ventricidal.

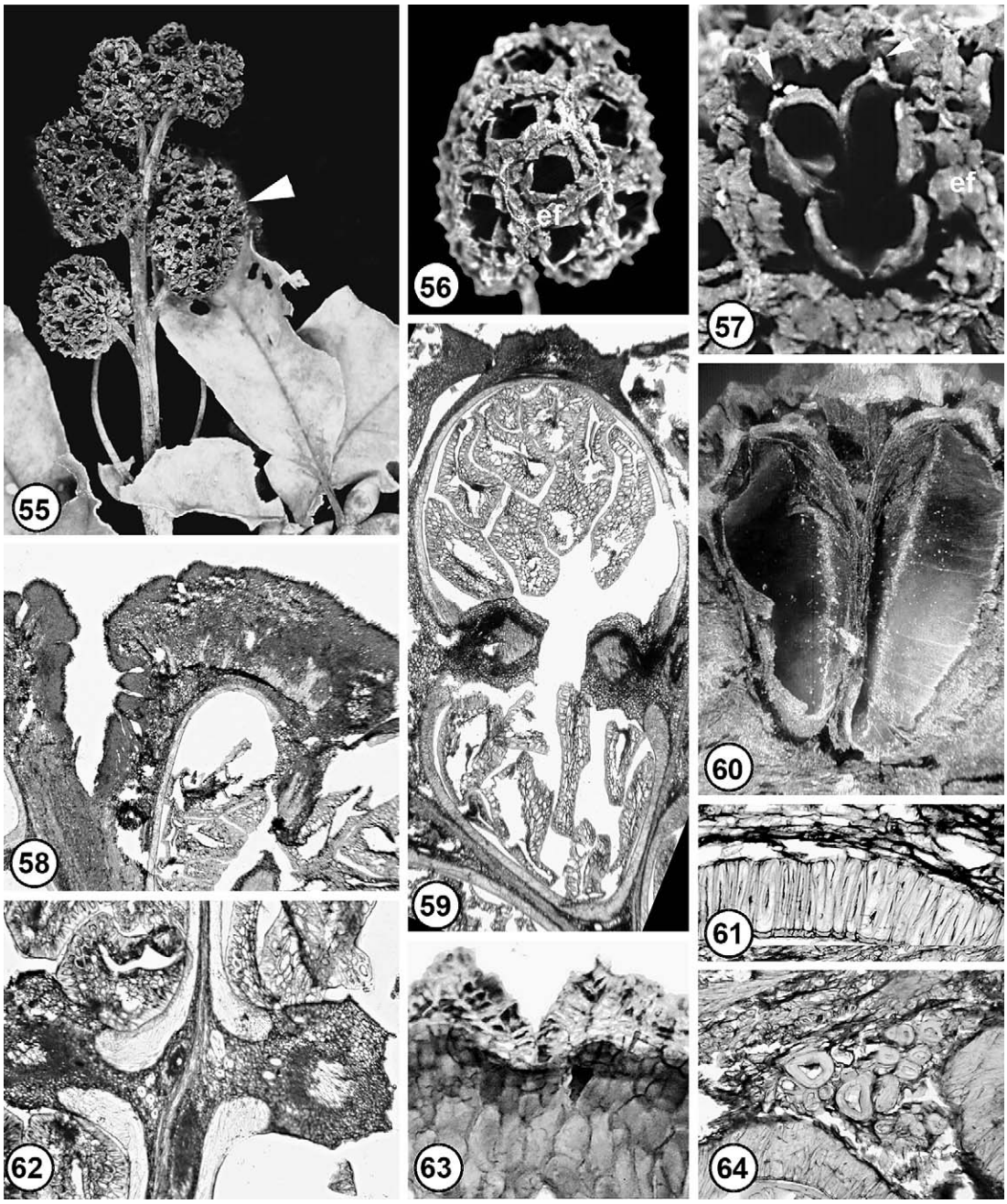

Figs. 55–64. *Altingia poilanei* infructescences. **55.** Fertile branch, showing distribution of turbinate infructescences. Note large aggregate infructescence (arrow), ×1.8. **56.** Mature infructescence showing mammilate tubercles of extrafloral processes (ef) between adjacent fruits, ×1.4. **57.** Detail of fruit showing unusual triloculate carpel and mammilate tubercles of extrafloral processes (ef). Note persistent style bases, appearing as small, light-colored areas (arrows) on tips of open carpels, ×2.9. **58.** Longitudinal section showing part of a biloculate fruit (bottom) and the expansion of extensive outer fruit wall with lobes, ×5.7. **59.** Transverse section (TS) of individual fruit at level showing common locule. Note padlike extensions of ventral carpel wall and numerous abortive ovules, ×8.4. **60.** Longitudinal hand-section revealing interior of locules, ×7.6. **61.** TS of uni- to biseriate, palisade, inner carpel wall of macrosclereids, with internal carpel tissues (above), ×42.9. **62.** Detail of ventral carpel walls of adjacent fruits, showing padlike extensions of ventral carpel wall, ×16.5. **63.** TS of outer fruit wall showing lenticel-like region, ×32.5. **64.** Detail of fruit near inner carpel wall showing thick-walled fibers with large lumina, ×28.3.

To better understand the actual process of dehiscence, we studied fruits and flowers of both *Liquidambar* and *Altingia* at several stages of development (Figs. 13–20). Dehiscence in Altingiaceae takes place via hygroscopic tension, which arises as each fruit wall dries out. Fruit walls tend also to break down tangentially, along planes of weakness, resulting in the common fractured appearance of fruits within the infructescence (Figs. 2, 26, 45, 56).

The fruit consists of two involute carpels (Bogle, 1986) (Figs. 13–20). The inner edges of the involute portion of the

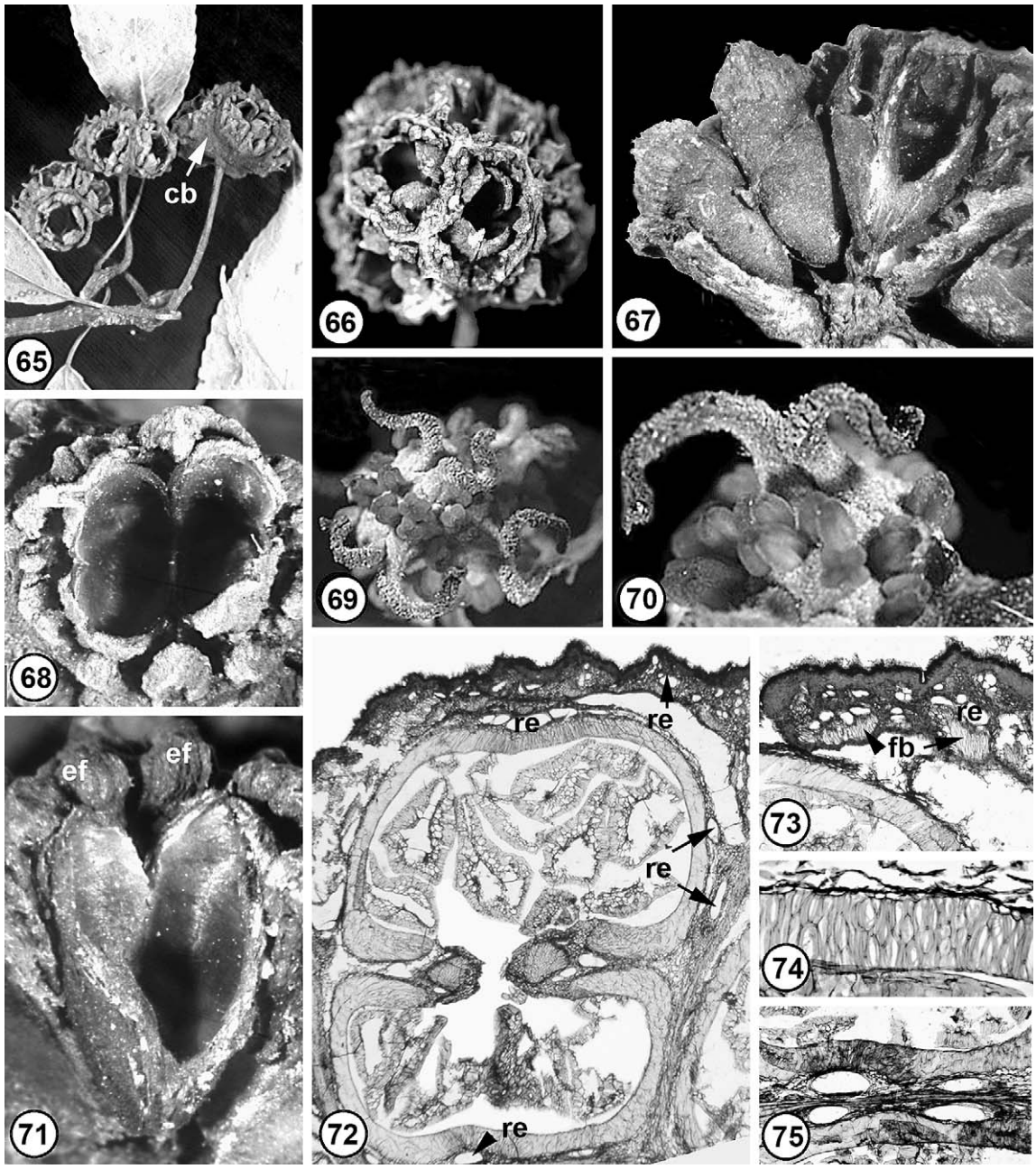

Figs. 65–75. *Altingia siamensis* infructescences and inflorescences. **65.** Mature infructescences showing few fruits per infructescence. Note cuplike bract (cb), ×1.2. **66.** Detail of mature fruit showing mammilate, irregular tubercles between adjacent fruits. Note persistent style bases (bottom), ×2.5. **67.** Longitudinal hand-section revealing outer fruit wall. Note that each fruit is separate and not tightly connected to adjacent fruits after drying and shrinking of floral tissues, ×5.3. **68.** Detail of dehiscence pattern with ventrally fused carpel margins. Style bases are not preserved, ×4.1. **69.** Inflorescence showing short, stout, recurved styles with broad, elongate stigmatic surfaces. Note stamens in center of inflorescence, ×5.8. **70.** Detail of recurved styles with elongate stigmatic surfaces and anthers at the bases of the styles, ×10.0. **71.** Longitudinal section through fruit showing inner carpel wall in surface view and mammilate ornamentation of extrafloral processes (ef; at top), ×7.4. **72.** Transverse section of an ovary at level with single common locule, ×11.6. **73.** Detail of outer fruit wall with prominent resin canals and arclike fiber bundle caps subtending resin canals. Note separation within outer fruit wall near the inner palisade layer, ×20.1. **74.** Detail of inner carpel wall made up of multiple layers of sclereids (up to four cells thick), ×22.3. **75.** Detail of tangentially elongate resin canals within inner fruit tissue, ×26.1.

ventral margins of each carpel are fused together, and the outer ventral margins of the two carpels composing the fruit are then fused to each other. (This entire structure produces the ventral septum sensu Bogle, 1986.) Centrally within the fruit the involute margins are fused to themselves ventrally and to each other, separating the two locules from one another (Figs. 19, 20). Distally, the lateral margins of each of the carpels split ventricidally, resulting in a large, common locule (Fig. 18). More distally, the two carpels are also separated from one another (Figs. 15–18).

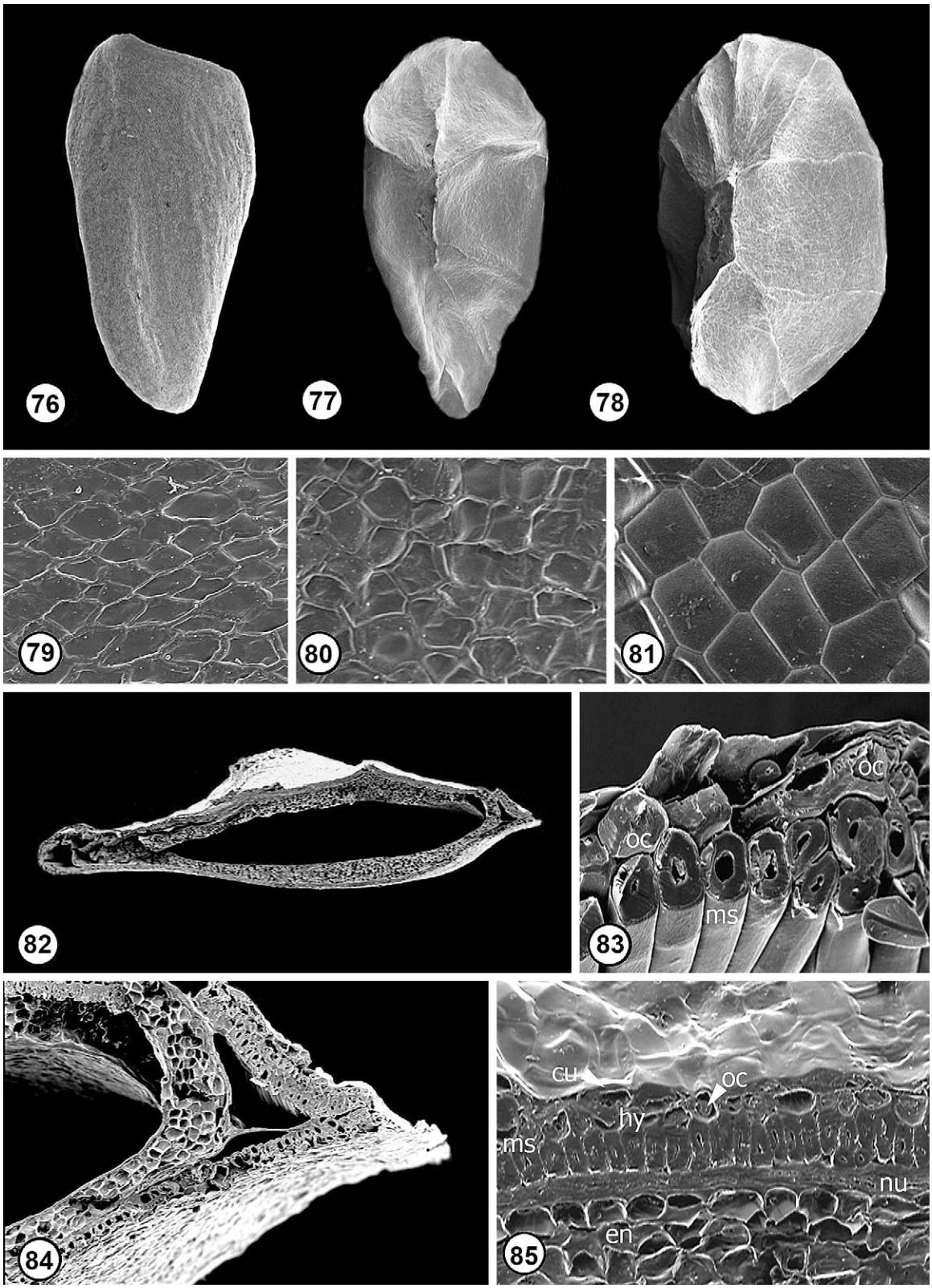

Figs. 76–85. SEM micrographs of seeds, seed coat micromorphology, and seed coat anatomy in *Altingia*. Figs. 76–78. Mature seeds. **76.** *Altingia siamensis*, ventral view of seed, ×9.2. **77.** Seed of *A. chinensis* with encircling flange. Note hilar scar (center), ×12.1. **78.** Seed of *A. poilanei* with encircling flange, note prominent hilar scar (left of center), ×6.8. **79.** *A. poilanei* seed coat surface with irregularly elongate polygonal cells, ×300. **80.** *A. siamensis* seed coat surface with somewhat angular, irregular polygonal cells, ×297. **81.** *A. excelsa* seed coat surface with highly geometric 4-, 5-, and 6-sided polygonal cells, ×750. **82.** Transverse section of *A. poilanei* seed showing lateral flanges of the encircling wing, ×23.4. **83.** Detail of the single layer

In fruits of *Liquidambar* and *Semiliquidambar*, the long, persistent styles not only obscure the view of the fruit openings but also help to maintain its structural integrity. Fruits of *Altingia* have only small remnants of style bases. Because *Altingia* fruits lack prominent styles, dehiscence is more pronounced, allowing the splitting of the bilocular fruits into four valves upon maturity as an additional loculicidal split does occur along the dorsal side of the carpel (Fig. 16). In *Liquidambar* and *Semiliquidambar*, the outer fruit wall is relatively thin, while in *Altingia* the wall is considerably thicker and more highly differentiated. In all altingioids, however, the drying that causes dehiscence also causes splitting of the fruit walls, allowing additional "room" for the fruits to open. As fruits mature and become desiccated, numerous fractures form throughout the ground tissues of the outer fruit walls.

A uniform terminology for dehiscence and a clearer understanding of the process are both essential to the value of this feature as a taxonomic character. Consistent terminology is also important when evaluating homologies and tracking character evolution within the group as a whole (Hermsen et al., 2006). Nowhere is it more important than in the study of the fossil record. In particular, the Eocene genus *Steinhauera* has been compared both to *Liquidambar* and *Altingia* (Kirchheimer, 1943, 1957; Mai, 1968). Mai (1968) contended that *Steinhauera*'s lack of persistent styles and possession of a fibrous axis demonstrated its closer relationship to *Altingia*, a genus that he suggested as basal within the family. This hypothesis has not been tested, and a reassessment of the numerous specimens of *Steinhauera* is needed. We do know, however, from our study of Miocene fossils that fruit weathering in extant *Liquidambar* can result in infructescences that look superficially like those of *Altingia* (Pigg et al., 2004). We are currently evaluating fossil Altingiaceae in this context.

Seed surface micromorphology in Altingiaceae—Seed surface micromorphology in *Altingia* is relatively homogenous with cells arranged parallel to the long axis of the seed (Figs. 76–81). In all species of *Altingia* and in *L. acalycina*, the surface of the seed coat is composed of polygonal cells (Figs. 79–81), while the other three species of *Liquidambar* have tangentially elongate and rectangular cells (Ickert-Bond et al., 2005). It is interesting to note that seeds of *Altingia* and *L. acalycina* have ovate seeds with a circular flange, while seeds of the other three species of *Liquidambar* have elongate seeds with a distal wing. Thus, epidermal cell pattern on seeds tend to correlate with seed shape in Altingiaceae.

Significance of seed anatomy in Altingiaceae—As with dehiscence, there have been difficulties in understanding the seed anatomy of Altingiaceae. Much of the difficulties arise because classification of seed anatomy is based on the developmental origin of the most mechanically prominent, usually sclerified, layer of the seed coat, and these relationships are not always obvious in mature seeds (Corner, 1976; Boesewinkel and Bouman, 1984; Schmid, 1986). Because most angiosperms are bitegmic, either the inner or outer integument provides the major mechanical layers of the seed coat. Seed coats developed primarily from the outer integument (testa) are termed testal, while those mostly from the inner integument (tegmen) are termed tegmic. The given region of the integument involved is included (e.g., mesotestal, endotegmic) in this classification (Corner, 1976).

Seed anatomy of Altingiaceae has been described by several authors (Netolitzky, 1926; Melikian, 1971, 1973; Rao, 1974; Takhtajan, 1996; Zhang and Wen, 1996). This feature has been interpreted variously as mesotestal (Corner, 1976), endotestal (Doweld, 1998), or exotegmic (Rao, 1974). As the ovule of Altingiaceae develops, the outer integument has 2–3 cell layers and the inner integument has 3–4 layers (Endress and Igersheim, 1999). In the mature seed, the outer integument of the ovule is represented by a layer only 2–5 cells thick. It is composed of the epidermis and a hypodermis with oxalate crystals (Figs. 9G–J in Ickert-Bond et al., 2005) (Figs. 76–85). From our observations, we interpret the thin, crushed, tangentially elongate layer (immediately outside the embryo cavity) and the mechanically prominent macrosclereids to the inside of this thinner layer as being derived from the inner integument (Fig. 85). In this case, the seeds of Altingiaceae would thus be considered exotegmic, because the mechanical layer comes from the tegmen. The innermost layer of crushed, tangentially elongate cells immediately outside the embryo cavity are thought to represent the nucellus.

In contrast, seed coats of Hamamelidaceae s.s. have been described as mesotestal, with the mechanical tissue derived from the middle layer of outer integument (Corner, 1976; Boesewinkel and Bouman, 1984), or exo-mesotestal, with this layer derived from both the outer and middle layers of the outer integument (Doweld, 1998). Developmentally, a mature hamamelid ovule has an outer integument 6–8 cells thick and an inner one of 2–3 cells (Endress and Igersheim, 1999). In the mature seed, the outer seed coat is massive and up to 30 cells thick, with centrally positioned sclerotic tissue, and the inner layers are considerably thinner (Rao, 1974; Zhang and Wen, 1996). This type of seed is thus classified as mesotestal. (Boesewinkel and Bouman, 1984; Schmidt, 1986).

In summary, Altingiaceae seed coats differ from those of Hamamelidaceae because they are exotegmic with relatively little cell division occuring during development. In contrast, Hamamelidaceae seeds have a massive sclerotic testa derived from an initially thick outer integument with considerable cell division having occurred to produce this mesotestal seed coat (Zhang and Wen, 1996). Thus seed coat, along with differences in pollen structure (Bogle and Philbrick, 1980; Zavada and Dilcher, 1986), wood anatomy (Sakala and Privé-Gill, 2004), and several other features mentioned herein, reinforce the recognition of Altingiaceae as an independent family distinct from the closely related Hamamelidaceae (Endress, 1989b; Ferguson, 1989; Ickert-Bond and Wen, 2006; Stevens, 2000 onward).

Comparison between morphological and molecular phylogenies within Altingiaceae—Analyses based on several molecular markers suggest that *Altingia* is nested within *Liquidambar* (Fig. 87) (Shi et al., 1998; Ickert-Bond et al., 2005; Ickert-Bond and Wen, 2006). Yet our morphological

←
of macrosclereids with small lumina in *A. chinensis*. Note oxalate druse crystals (oc) in the hypodermis, ×528. **84.** Detail of Fig. 82 (at right) showing tissue layers of seed coat, ×123. **85.** Seed coat of *A. siamensis* showing thick cuticle (cu) on epidermis. Note druse crystals (oc) in the hypodermis (hy), above the thick-walled macrosclereids (ms), crushed cells of nucellar tissue (nu) above parenchymatous endosperm (en), ×595.

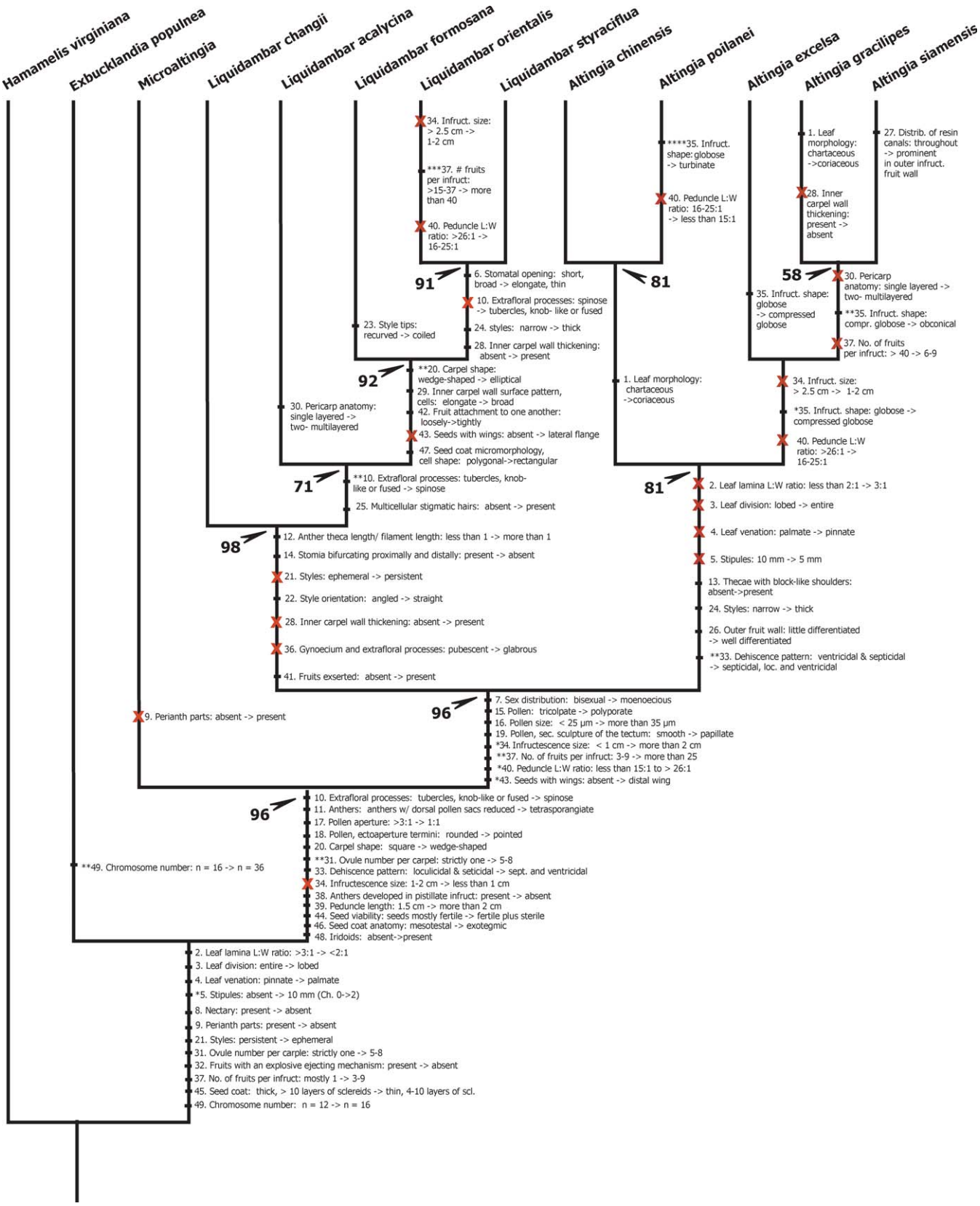

Fig. 86. Phylogenetic relationships among Altingiaceae based on morphology using parsimony. Tree shown is the single most parsimonious tree. Numbers next to arrows reflect bootstrap support values. Most character changes are changes from 0 to 1; other changes are specifically marked: *, changes from 0 to 2; **, changes from 1 to 2; ***, changes from 2 to 3; ****, changes from 0 to 3; and reversals are marked by an "X" on the phylogeny.

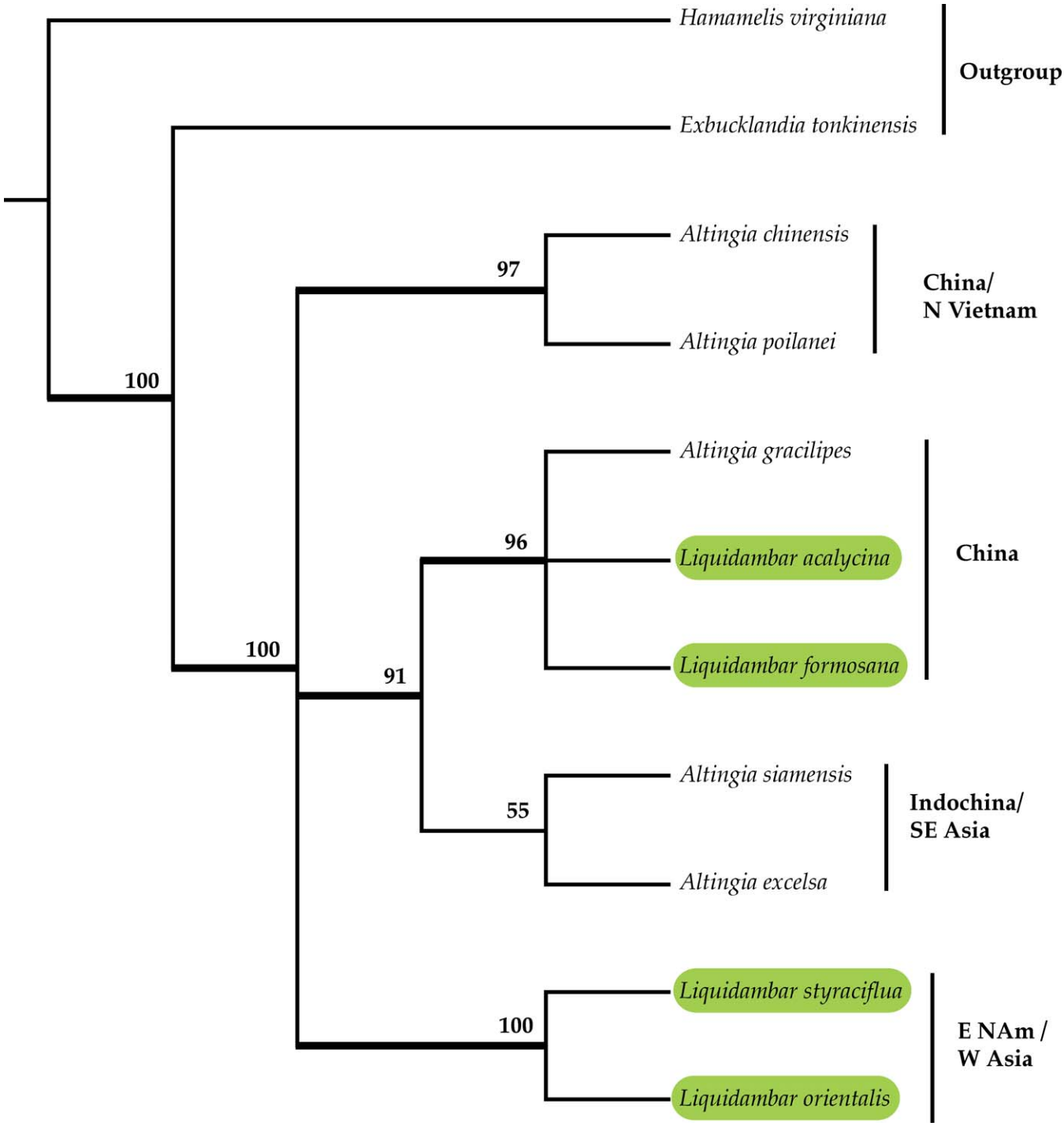

Fig. 87. Phylogenetic relationships among Altingiaceae based on maximum parsimony analysis of combined *cp*DNA data (*trnL-trnF* IGS, the *psaA-ycf3* IGS, the *rps16* intron, the *trnS-trnG* IGS, and the *trnG* intron; modified from Ickert-Bond and Wen, 2006). Strict consensus tree shown, with numbers above branches reflecting bootstrap values.

analysis strongly supports *Altingia* and *Liquidambar* as mutually exclusive sister clades (Fig. 86) (Ickert-Bond et al., 2005). The Cretaceous fossil *Microaltingia* is supported as sister to the Altingiaceae within the stem lineage of Altingiaceae (Fig. 86) (Ickert-Bond and Wen, 2006). Results in Hermsen et al. (2006) place *Microaltingia* below a clade of Altingiaceae and place *Cercidiphyllum* L. slightly further from Altingiaceae, as originally proposed in Zhou et al. (2001). *Liquidambar* and *Altingia* are each defined by several morphological synapomorphies and have been maintained as separate genera in modern taxonomic treatments (Vink, 1957; Tardieu-Blot, 1965; Zhang et al., 2003). The apparent

TABLE 5. Infructescence morphology and dehiscence types reported for Altingiaceae by different authors.

Taxon	Authors				
	Kirchheimer (1957)	Mai (1968)	Ferguson (1989)	Endress (1989a)	Zhang et al. (2003)
Altingia	Septicidal & loculicidal	Septicidal & loculicidal	Septicidal & loculicidal	Septicidal & loculicidal	Dehiscing loculicidally by two 2-lobed valves
Semiliquidambar	—	—	Septicidal dehiscence	—	Dehiscing by two 2-lobed valves
Liquidambar	Septicidal	Septicidal, seldom loculicidal	Septicidal dehiscence	Ventricidal (follicular) & septicidal	Loculicidally by 2 valves
Steinhauera	Septicidal	Septicidal & loculicidal, predominantly septicidal	Septicidal and loculicidal	Septicidal and loculicidal	—

incongruence of these phylogenies appears to be due to discordant rates of evolution in molecules and morphology as well as morphological convergence.

The five species of *Altingia* are morphologically distinct. For example, *A. gracilipes* and *A. siamensis* are easily distinguished from the other three species (*A. chinensis*, *A. excelsa*, and *A. poilanei*) by having only few fruits per small infructescence and a distinct cuplike bract subtending the fruits (Table 3). While both *A. chinensis* and *A. poilanei* have relatively thick peduncles and thick coriaceous leaves, *A. excelsa* has thinner peduncles and chartaceous leaves. Long, thick peduncles bearing medium-sized fruits set *A. chinensis* apart from *A. poilanei*, which has larger fruits borne on much shorter peduncles.

Molecular divergence is lower in *Altingia* than in *Liquidambar*: the average chloroplast DNA (*trnL-trnF* intergenic spacer [IGS], the *psaA-ycf3* IGS, the *rps*16 intron, the *trnS-trnG* IGS, and the *trnG* intron) pairwise sequence divergence is 0.02% (0–0.4% in range) in *Altingia* but 0.6% (0–0.9% in range) in *Liquidambar* (Ickert-Bond and Wen, 2006).

The discordance between morphological and molecular divergence rates seems to be linked with habitat preferences of species, which have been noted in other groups as well (Moritz et al., 2000; Buzas et al., 2002; Lecompte et al., 2005), including species that have undergone recent adaptive radiations, such as columbines (Hodges and Arnold, 1994) and Hawaiian silverswords (Baldwin and Robinchaux, 1995).

Character-state changes in *Altingia* seem to correlate with tropical and subtropical environments in eastern Asia and Indochina whereas changes in *Liquidambar* correlate with temperate sites, where the genus is found today. Of the eight characters defining *Altingia*, four are reversals (characters 2–5: ratio of leaf length to width, leaf division, venation, and stipule size) (Fig. 86). Three characters are synapomorphies without homoplasies (character 13, theca shape; character 26, outer fruit wall; and character 33, dehiscence type), and one (character 24, style shape) converges. The availability of diverse habitats in tropical and subtropical eastern Asia and Indochina facilitated the diversification of *Altingia* species in response to recent active uplifts of mountains in eastern Asia since the Tertiary (Morley, 1999; Wen, 1999, 2001).

In the morphological analysis, characters that distinguish *Liquidambar* from *Altingia* are related to an open wind pollination syndrome and may represent convergences to temperate habitats. *Liquidambar* is supported by seven synapomorphies (Fig. 86): (1) filaments longer than anthers (character 12); (2) absence of stomium bifurcations (character 14); (3) persistent styles (character 21); (4) straight styles (character 22); (5) cells of inner carpel wall thickened (character 28); (6) glabrous gynoecium (character 36); and (7) exserted fruits (character 41). In particular, the presence of anthers borne on long filaments and the loss of stomium bifurcations would facilitate the wind dispersal of pollen (Hufford and Endress, 1989), while long narrow styles on exserted fruits may aid in the capture of pollen on the broad stigmatic surfaces in open habitats of temperate *Liquidambar*.

In contrast to *Altingia, Liquidambar* appears to be delimited by several synapomorphies related to wind pollination (e.g., long filaments, exserted fruits). However, at a higher node within the genus (above *L. acalycina*), a second set of synapomorphies may also represent adaptations for a temperate distribution. These characters (elongate and tapered carpel shape, seeds with distal wings, and more tightly constructed infructescences [Fig. 86]) are related to seed rather than pollen dispersal. Several other families (e.g., Platanaceae) show a similar convergence among temperate members (Tiffney, 1984; Crane, 1989).

At a higher node still, the species pair *Liquidambar styraciflua* and *L. orientalis* are highly convergent, particularly in the clinal variation of leaves (5–7 lobes) to the extent that some authors have suggested the two species may be conspecific (Reichinger, 1943; Meikle, 1977). Similarities include thick styles (character 24), thickened cells of the inner carpel wall (character 28), a lack of spine-like extrafloral processes (character 10), and elongate and thin stomatal openings (character 6). They differ in infructescence size (character 34), number of fruits per infructescence (character 37), and peduncle L : W ratio (character 40).

The genetic variability between the two species is, however, greater than morphology would suggest. Based on isozymes, these two species were estimated to have diverged from one another in the Middle Miocene (ca 13 mya ago; Hoey and Parks, 1991). Our molecular studies confirm these findings, with the two species having a cpDNA sequence divergence of 0.65%. Divergence time was estimated to be 22.90 $\pm$ 10.24 mya, or as old as early Oligocene (33 mya) or as late as middle Miocene (13 mya) (Ickert-Bond and Wen, 2006); during this period, the northern hemisphere experienced a temperate climate (Graham, 1999). The deep molecular divergence coupled with the high level of morphological similarity suggests a conserved morphology of these two taxa (Figs. 86, 87), i.e., morphological stasis, an evolutionary phenomenon that has been proposed for many animal groups as well as some plant taxa (reviewed in Wen, 1999; Ickert-Bond et al., 2005; Eldredge et al., 2005; Graham, 2006; Nie et al., 2006).

Differences in rates of evolution and morphological

convergence suggest complex patterns of diversification in Altingiaceae at several different phylogenetic levels: (1) at deep nodes, morphological stasis is indicated because characters of the the stem lineage in Cretaceous *Microaltingia* also occur in the crown group; (2) at the generic level, convergence within the primarily temperate genus *Liquidambar* and within the Asian tropical to subtropical genus *Altingia*; (3) at the infrageneric level, morphological divergence within *Altingia*, in response to habitat diversity in the subtropics of eastern Asia; and (4) in the intercontinental disjunct species pair *L. orientalis–L. styraciflua*, morphological stasis. Future analysis is needed to quantify morphological diversification rates comparatively between *Altingia* and *Liquidambar*. Understanding the evolutionary diversification of plants in the context of geography and time will enable us to further test the hypothesis of morphological stasis in temperate plants.

LITERATURE CITED

ARCHIE, J. W. 1985. Methods for coding variable morphological features for numerical taxonomic analysis. *Systematic Zoology* 34: 326–345.

BALDWIN, B. G., AND R. H. ROBINCHAUX. 1995. Historical biogeography and ecology of the Hawaiian silversword alliance (Asteraceae): new molecular phylogenetic perspectives. *In* W. L. Wagner and V. A. Funk [eds.], Hawaiian biogeography: evolution on a hot spot archipelago, 259–299. Smithsonian Institution Press, Washington, D.C., USA.

BOESEWINKEL, F. D., AND F. BOUMAN. 1984. The seed: structure. *In* B. M. Johri [ed.], Embryology of angiosperms, 567–610. Springer-Verlag, Berlin, Germany.

BOGLE, A. L. 1986. The floral morphology and vascular anatomy of the Hamamelidaceae: subfamily Liquidambaroideae. *Annals of the Missouri Botanical Garden* 73: 325–347.

BOGLE, A. L., AND C. T. PHILBRICK. 1980. A generic atlas of hamamelidaceous pollens. *Contributions from the Gray Herbarium of Harvard University* 210: 29–103.

BUZAS, M. A., L. S. COLLINS, AND S. J. CULVER. 2002. Latitudinal difference in biodiversity caused by higher tropical rate of increase. *Proceedings of the National Academy of Sciences, USA* 99: 7841–7843.

CARLQUIST, S. 1982. The use of ethylene diamine in softening hard plant tissue for paraffin sectioning. *Stain Technology* 57: 311–317.

CHANG, H.-T. 1962. *Semiliquidambar*, novum Hamamelidacearum genus *Sinicum*. *Sunyatsen University Bulletin of Natural Science* 1: 34–44.

CHANG, H.-T. 1979. Hamamelidaceae. *In* H.-T. Chang [ed.], Flora Reipublicae Popularis Sinicae, vol. 35, no. 2, 36–166. Science Press, Beijing, China.

CHENG, W-C. 1947. New Chinese shrubs and trees. *Forestry Institute, National Central University, Nanking, Research Notes, Dendrological Series* 1: 1–4.

CORNER, E. J. H. 1976. The seeds of dicotyledons, vol. 1. Cambridge University Press, Cambridge, UK.

CRAIB, W. G. 1928. Contributions to the flora of Siam. *Kew Bulletin* 1928: 68.

CRANE, P. R. 1989. Paleobotanical evidence on the early radiation of nonmagnoliid dicotyledons. *Plant Systematics and Evolution* 162: 165–191.

DOWELD, A. B. 1998. Carpology, seed anatomy and taxonomic relationships of *Tetracentron* (Tetracentraceae) and *Trochodendron* (Trochodendraceae). *Annals of Botany* 82: 413–443.

ELDREDGE, N., J. N. THOMPSON, P. N. BRAKEFIELD, S. GRAVRILETS, D. JABLONSKI, J. B. C. JACKSON, R. E. LENSKI, B. S. LIBERMAN, M. A. MCPEEK, AND W. MILLER III. 2005. Dynamics of evolutionary stasis. *Paleobiology* 3: 133–145.

ENDRESS, P. K. 1989a. Aspects of evolutionary differentiation of the Hamamelidaceae and the lower Hamamelididae. *Plant Systematics and Evolution* 162: 193–211.

ENDRESS, P. K. 1989b. A suprageneric taxonomic classification of the Hamamelidaceae. *Taxon* 38: 371–376.

ENDRESS, P. K. 1993. Hamamelidaceae. *In* K. Kubitzki [ed.], The families and genera of vascular plants, vol. 2, Flowering plants, dicotyledons, 322–330. Springer-Verlag, Berlin Heidelberg, Germany.

ENDRESS, P. K., AND A. IGERSHEIM. 1999. Gynoecium diversity and systematics of the basal eudicots. *Botanical Journal of the Linnean Society* 130: 305–393.

ESAU, K. 1965. Plant anatomy. Wiley, New York, USA.

FELSENSTEIN, J. 1985. Confidence limits on phylogenies: an approach using the bootstrap. *Evolution* 39: 783–791.

FERGUSON, D. K. 1989. A survey of the *Liquidambaroideae* (Hamamelidaceae) with a view to elucidating its fossil record. *In* P. R. Crane and S. Blackmore [eds.], Evolution, systematics, and fossil history of the Hamamelidae, vol. 1, 249–272. Systematics Association special volume no. 40A. Clarendon Press, Oxford, UK.

FERGUSON, D. K. 2002. *Altingia siamensis*, an apomorphic member of the Altingiaceae. 12th Flora of Thailand Meeting, 2002, 27. National Park, Wildlife and Plant Conservation Department, Bangkok, Thailand. Website http://www.dnp.go.th/botany/Image/events/Flora%20meeting/abstract.htm [accessed 2 July 2006].

GRAHAM, A. 1999. Late Cretaceous and Cenozoic history of North American vegetation. Oxford University Press, Oxford, UK.

GRAHAM, A. 2006. Paleobotanical evidence and molecular data in reconstructing the historical phytogeography of Rhizophoraceae. *Annals of the Missouri Botanical Garden* 93: 325–334.

HERMSEN, E. J., K. C. NIXON, AND W. L. CREPET. 2006. The impact of extinct taxa on understanding the early evolution of angiosperm clades: an example incorporating fossil reproductive structures of Saxifragales. *Plant Systematics and Evolution* 260: 141–169.

HODGES, S. A., AND M. ARNOLD. 1994. Columbines: a geographically widespread species flock. *Proceedings of the National Academy of Sciences, USA* 91: 5129–5132.

HUFFORD, L. D., AND P. K. ENDRESS. 1989. The diversity of anther structure and dehiscence patterns among Hamamelididae. *Botanical Journal of the Linnean Society* 99: 301–346.

ICKERT-BOND, S. M., K. B. PIGG, AND J. WEN. 2005. Comparative infructescence morphology in *Liquidambar* (Altingiaceae) and its evolutionary significance. *American Journal of Botany* 92: 1234–1255.

ICKERT-BOND, S. M., AND J. WEN. 2006. Phylogeny and biogeography of Altingiaceae: evidence from combined analysis of five non-coding chloroplast regions. *Molecular Phylogenetics and Evolution* 39: 512–528.

JOHANSEN, D. A. 1940. Plant microtechnique. McGraw Hill, New York, New York, USA.

KIRCHHEIMER, F. 1943. Über *Steinhauera subglobosa* Presl. und die Reste von *Liquidambar*-Fruchtständen aus dem Tertiär Mitteleuropas. *Neues Jahrbuch für Mineralogie, Geologie und Paläontologie Monatshefte, Abteilung. B, Heft* 8/9: 216–236.

KIRCHHEIMER, F. 1957. Die Laubgewächse der Braunkohlenzeit. VEB Wilhelm Knapp Verlag, Halle (Salle), Germany.

LECOMPTE, E., C. DENYS, AND L. GRANJON. 2005. Confrontation of morphological and molecular data: the *Praomys* group (Rodentia, Murinae) as a case of adaptive convergences and morphological stasis. *Molecular Phylogenetics and Evolution* 37: 899–919.

LOBOVA, T. A., A. M. SCOTT, F. BLANCHARD, H. PECKHAM, AND P. CHARLES-DOMINIQUE. 2003. *Cecropia* as a food resource for bats in French Guiana and the significance of fruit structure in seed dispersal and longevity. *American Journal of Botany* 90: 388–403.

MAI, H. D. 1968. Zwei ausgestorbene Gattungen im Tertiär Europas und ihre florengeschichtliche Bedeutung. *Palaeontographica* 123B: 184–199.

MEIKLE, R. D. 1977. Flora of Cyprus, vol. 1. Betham-Moxum Trust, Royal Botanical Gardens, Kew, UK.

MELIKIAN, A. P. 1971. The anatomical structure of the spermoderm of the representatives of the genera *Liquidamabar* L. and *Altingia* Nor. relative to its systematics. *Biologicheski Zhurnal Armenii* 24: 50–55.

MELIKIAN, A. P. 1973. Seed coat types of Hamamelidaceae and allied

families in relation to their systematics. *Botaneski Zhurnal* 58: 350–359.

MERRILL, E. D., AND W.-Y. CHUN. 1935. Hainan plants. *Sunyatsenia* 2: 238.

MORITZ, C., J. L. PATTON, C. J. SCHNEIDER, AND T. B. SMITH. 2000. Diversification of rainforest faunas: an integrated approach. *Annual Reviews in Ecology and Systematics* 31: 533–563.

MORLEY, R. J. 1999. Origin and evolution of tropical rainforests. Wiley, Chichester, UK.

NETOLITZKY, F. 1926. Anatomie der Angiospermen-Samen. Handbuch der Pflanzenanatomie. II. Abteilung, 2. Teil: Pteridophyten und Anthophyten. Verlag von Gebrueder Borntraeger, Berlin, Germany.

NIE, Z.-L., H. SUN, P. M. BEARDSLEY, R. G. OLMSTEAD, AND J. WEN. 2006. Evolution of biogeographic disjunction between eastern Asia and eastern North America in *Phyrma* (Phyrmaceae). *American Journal of Botany* 93: 1343–1356.

PIGG, K. B., S. M. ICKERT-BOND, AND J. WEN. 2004. Anatomically preserved *Liquidambar* (Altingiaceae) from the Middle Miocene of Yakima Canyon, Washington State, USA, and its biogeographic implications. *American Journal of Botany* 91: 499–509.

RAO, R. P. M. 1974. Seed anatomy in some Hamamelidaceae and phylogeny. *Phytomorphology* 24: 113–139.

REICHINGER, K. H. 1943. Flora Aegaea. Flora der Inseln und Halbinselsn des Ägäischen Meeres. Akademie der Wissenschaften in Wien. *Mathematisch-Naturwissenschaftliche Klasse, Denkschriften* 105: 1–924.

SAKALA, J., AND C. PRIVÉ-GILL. 2004. Oligocene angiosperm woods from Northwestern Bohemia, Czech Republic. *International Association of Wood Anatomists Journal* 25: 369–380.

SCHMIDT, R. 1986. On Cornerian and other terminology of angiospermous and gymnospermous seed coats: historical perspective and terminological recommendations. *Taxon* 35: 476–491.

SHI, S., Y. HUANG, H.-T. CHANG, Y. CHEN, L. QU, AND J. WEN. 1998. Phylogeny of the Hamamelidaceae based on ITS sequences of nuclear ribosomal DNA. *Biochemical Systematics and Ecology* 26: 55–69.

STEVENS, P. F. 2000 onward. Angiosperm phylogeny website, version 6, 22 May 2006 [and more or less continuously updated since]. Website http://www.mobot.org/MOBOT/research/APweb/ [accessed 19 June 2006].

STOPP, K. 1950. Karpologische Studien I und II. Vergleichend-morphologische Untersuchungen über die Dehiszensformen der Kapselfrüchte. *Abhandlungen der Mathematisch-Naturwissenschaftlichen Klasse, Akademie der Wissenschaften und der Literatur, Mainz* 7: 165–210.

SWOFFORD, D. I. 2002. PAUP*: phylogenetic analysis using parsimony (*and other methods), version 4b. Sinauer, Sunderland, Massachusetts, USA.

TAKHTAJAN, A. 1996. Anatomia seminum comparativa, vol. 5. Nauka, Leningrad, Russian Federation.

TARDIEU-BLOT, M. L. 1965. Hamamelidaceae. *In* A. Aubréville and M. L. Tardieu-Blot [eds.], Flore du Cambodge du Laos et du Vietnâm, fascicle 4, 75–116. Muséum National d'Histoire Naturelle, Paris, France.

TIFFNEY, B. H. 1984. Seed size, dispersal syndromes, and the rise of the angiosperms, evidence and hypotheses. *Annals of the Missouri Botanical Garden* 71: 551–576.

VINK, W. 1957. Hamamelidaceae. *In* C. G. J. van Steenis [ed.], Flora Malesiana, vol. 5. Nationaal Herbarium, Leiden, Netherlands.

WEN, J. 1998. Evolution of eastern Asian and eastern North American disjunct pattern: insights from phylogenetic studies. *Korean Journal of Plant Taxonomy* 28: 63–81.

WEN, J. 1999. Evolution of the eastern Asian–eastern North American biogeographic disjunctions in flowering plants. *Annual Review of Ecology and Systematics* 30: 421–455.

WEN, J. 2001. Evolution of eastern Asian–eastern North American biogeographic disjunctions: a few additional issues. *International Journal of Plant Sciences* 162: S117–S122.

WINKLER, H. 1936. Septizide Kapsel und Spaltfrucht. *Beiträge zur Biologie der Pflanzen* 24: 191–200.

ZAVADA, M. S., AND D. L. DILCHER. 1986. Comparative pollen morphology and its relationship to phylogeny of pollen in the Hamamelidae. *Annals of the Missouri Botanical Garden* 73: 348–381.

ZHANG, Z. Y., AND J. WEN. 1996. The seed morphology in Hamamelidaceae and its systematic evaluation. *Acta Phytotaxonomica Sinica* 34: 538–546.

ZHANG, Z. Y., H.-T. ZHANG, AND P. K. ENDRESS. 2003. Hamamelidaceae. *In* Z.-Y. Wu, P. H. Raven, and D.-Y. Hong [eds.], Flora of China, vol. 9, 18–42. Science Press, Beijing, China.

ZHOU, Z.-K., W. L. CREPET, AND K. C. NIXON. 2001. The earliest fossil evidence of the Hamamelidaceae: late Cretaceous (Turonian) inflorescences and fruits of Altingioideae. *American Journal of Botany* 88: 753–766.

APPENDIX. List of examined specimens. Specimens from the same locality are separated by commas. Voucher specimens from the following herbaria have been examined: A, Arnold Arboretum of Harvard University; ASU, Arizona State University; E, Royal Botanic Garden, Edinburgh; F, Field Museum of Natural History; GH, Gray Herbarium of Harvard University; MO, Missouri Botanical Garden; NY, The New York Botanical Garden; and P, Muséum National d'Histoire Naturelle, Laboratoire de Phanérogamie, Paris. Taxon—*COUNTRY*. **State**: Locality, *Voucher* specimen (Herbarium).

Altingia Noronha, section Altingia

***A. chinensis* (Champion ex Bentham) Oliver ex Hance (= *A. obovata* Merrill et Chun)—*CHINA*. Guangdong**: Guangdong Institute of Forestry, *Hao 923* (ASU); Ruyuan Xian, *C. Wang 44102* (MO); Lokchong, *C. L. Tso 21049* (E); Poon Yue district, *C. O. Levine 3158* (MO); Naam Kwan Shan, Tsengshing District, *W. T. Tsang 20218* (E, MO, P); Heping County, Reshui, *Ickert-Bond 1343* (F); Lin Fa Shan, Sam Hang Shek T'au Village, Hwei-yang District, *W. T. Tsang 25942* (A, E); Xinyi Xian, *C. Wang 31828* (MO); Kwai Shan, Tsing-lo-kong village, Ho-yuen district, *W. T. Tsang 28544* (A); South China Botanical Garden, *Hao 920* (ASU); Nanling National Forest Park, Ickert-Bond 1303 (F). **Guangxi**: Shap Man Taai Shan, near Hoh Lung village, SE of Shang-ze, Guangdong border (Shang-ze district), *W. T. Tsang 22577* (A); She-Feng Dar Shan, S. Nanning, *R.-C. Ching 7937* (A); Tong Shan (along Guangdong border), near Sap-luk Po village (Waitsap district), *W. T. Tsang 22788* (A); Chen Pien District, *S. P. Ko 56024* (A); Shap Man Taai Shan, near Iu Shan village, SE of Shang-ze, Guangdong border, Shangze district, *W. T. Tsang 22189* (A); Pingnan Xian, *C. Wang 39334* (MO); Foo Lung, Sup Man Ta Shan, *H. Y. Liang 69714* (A). **Guizhou**: [Kweichow (S)], border of Guangxi [Kwangsi], Waichai, Dushan county, *Y. Tsiang 6677* (E). **Hainan**: Qiong Zhong county, Cheng Po district, Da Li village, Baishui Ling, *L. Deng 3685* (MO); no specific locality, *C. Wang 35691* (MO); Ding'an Xian, *C. Wang 36153* (MO); Hainan, Lingshui Xian, *C. Wang 36638* (MO); Ledong County, Jianfeng Natural Reserve, *Ickert-Bond 1372* (F); Diaoluo Mts. National Forest Park, Lingshui County, *Ickert-Bond 1362* (F); no specific locality, *H. Y. Liang 64371* (E), *64734* (GH), *62594* (P); Mo San Leng, *N. K. Chun 44321* (GH); no specific locality, *C. Wang 35897* (GH); Waning County, Liulian Mts., *Y. Zhong 4321* (MO); Waning county, Wumie district, Tongtie mountain (Ling), *Z. Li 4972* (GH). **Hong Kong**: no specific locality, *C. Wright 185* (A); Lokchong, *C. L. Tso 21049* (E); Sha Tau Kok-Luk Keng, *S. Y. Hu 9989* (A); Jardin Botanique, *E. Bodinier 1042* (E); Hong Kong Botanical Garden, *S. Ickert-Bond 1274* (F); Shing Mun Country Park, Shing Mun Arboretum, *S. Ickert-Bond 1261* (F). **Taiwan**: Lai Long Wan, Saikeng, *S. Y. Hu 47* (A). **Zhejiang**: Feng Yang Mtn., *H.-Y. Zou 307* (A), *761* (MO). *VIETNAM*. **Lao Cai**: Sa Pa, *A. Petelot 2332* (A, MO), *5944* (A); *M.Brillet 19* (P, 2 sheets).

***A. excelsa* Noronha—*BHUTAN*.** Sarbhang district: above Noonpani, 16 km along Sarbhang-Chirang road, *A. Grieson 3581* (E). *CHINA*.

Yunnan: Ping-pien Hsien, *H. T. Tsai 61528* (GH); Shweli valley, *G. Forrest 8763* (3 sheets, E, GH); between Tengyueh and Lungling, *J. F. Rock 7174* (GH); between Muang Hing and Szemao and the Szemao hills proper, Southern Yunnan, *J. F. Rock 2768*; no specific locality, *G. Forrest 18414* (GH, NY). *INDIA*. East Bengal, Griffith 3380 (3 sheets, A, GH, P); across river SE of Paungdaw Power Station, Gowahatti, *King s.n.* (A); Lakhimpur, Assam, collector 15189 (E); Jingale Bam near Nagahill, *Prain 769* (GH); Kachin Hills, Saden, Upper Burma, Mokim, *Shaik s.n.*; Ind. Or., *Griffith 286* (GH); Ceylon, Royal Botanic Gardens, Peradeniya, sect. C 276, *D. M. A. Jayaweera 1617* (GH). *INDONESIA*. East Timor, Koepang, *De Voogd 1772* (A); N. Sumatra, Karo plateau, Kaban Djahe, *J. A. Loerzing 17368* (A); West-Java, Res. Batavia. Pasir Tjarewed, Land Boland, west of Bogor (Buitenzorg), elev. 600 m., *Bakhuizen 6372* (MO); Dutch West Indies, *van de Koppel 3299* (MO); Bali Timur, Tabana. 2 km W of Candi Kuning, in natural areas of Kebun Raya, beyond introduced Altingia forest, *McDonald 4966* (2 sheets, E, GH); Java, *Field Museum 373260* (A); W. Java, Nirmala Estate, gu Halimum area, Blukar and remnant of forest, *Balgooy, M. M. J. v., 2912* (GH); South East Java, *H. O. Forbes 1201* (GH); Java, Ijoboshan, *C. S. Sargen s.n.* (GH); Sumatra, Res. Benkaelen and Afd. Redjang, *T. H. Endert 1068* (A); Sumatra, Sumatra's Westk. *Moera-Laboch For. Serv, Neth. Ind. 18066* (GH). *MYANMAR*. Patkai Mts., *G. Schaap 13* (A); gorge of the Hkrang Hka, North Triangle (Hkinhum), *F. Kingdon-Ward 20761* (A); Tenasserim Division, Tavoy District, *J. Keenan 1940* (A); east of Paungdaw Power Station, west bank of the Paungdaw chaung, *J. Keenan 1407* (E); south of Hpuginhku village, *J. Keenan 3679* (E). *THAILAND*. NE Kjonkaen, Phu Khieo, Game Reserve, ca. 80 km E of Phetchabun, *Kyoto University 41655* (A); Nakhon Nayok, Khao Yai National Park, *T. Smitinand 10848* (E). *MALAYSIA*. Malaya, Mentigi Forest Reserve, Cameron Highlands, *Bogle 313* (ASU).

***A. poilanei Tardieu-Blot*—*VIETNAM*. Lao Cai**: Lao Cai, Vietnam, Ta Phing prés de SaPa, *M. Poilane 12844* (P); Ta Phing Hmong village, some of the last remaining forest by small river across from rice paddies, *S. Ickert-Bond 1296* (F).

Altingia Noronha, section Oligocarpa

A. siamensis Craib. (= *A. takhtajanensis* Thai Van Trung & Lie Viet Lok)—*CAMBODIA*. Forét de Phnom Penh, Komnhan, *M. Bejaud 877* (P). **Kampot**: Bokor National Park, Pokopvil waterfall near the head, *S. Ickert-Bond 1280, 1281* (F); Kampot, Bokor National Park, upper Popovill waterfall head, *M. Monyrak 10* (A). *INDONESIA*. Java, Preanger Takoka, *Koordes 15754B* (P). *LAOS*. Fam Neva et M. Ham, *M. Poilane 2000* (2 sheets, A, P); haut cours de la Zehepone entre A Chieng et Klem Zalo, *M. Poilane 13500* (P); Pak Song, Sedone Prov., Sedone, *J. E. Vidal 4461* (P). *THAILAND*. Khao Yai, *Hardial 601* (A); Nam Phnom, Prov. E., District Chaiyaphum, *C. F. van Beusekom 4102* (MO). *VIETNAM*. Semi flumen Da one in foret Bieu Loa, *L. Pierre s.n.* (P); Cay to hop, Nhatrang, *M. Poilane 3228* (P); Ka Rom pro: Phanrang, *M. Poilane 9938* (2 sheets, P); Tourane, 100 km S of Hue, the later being Loureiro's type locality for the majority of the Cochinchina species, *J. Clemens 3388* (3 sheets, A, MO, P); en peu au sud de la Mation agricole de Blao prês du Haut Donai, *M. Poilane 22153* (P).

***A. gracilipes Hemsley*—*CHINA*. Fujian**: *Dunn 2682* (GH). **Guangdong**: Chaochow district, *N. K. Chun 42718* (MO); Heping County, Reshui, *Ickert-Bond 1344* (F); Yunfu Xian, *C. Wang 37057* (MO); Raoping Xian, *N. K. Chun 42718* (MO); Tung Koo Shan, Tapu district, Tan Shue, *W. T. Tsang 21697* (2 sheets, GH, P); Yam Na Shan [Yit Nga Shan] Mei [Kaying] District, *W. T. Tsang 21514* (GH); Nam Chung, *T. W. Lau 98* (GH); Nam Chung, *D. Lau 43* (GH). **Hong Kong**: Sha Tau Kok-luk Keng, *S. Y. Hu 9984* (GH); Pat Sin Leng Country Park, Nam Chung trail, *S. Ickert-Bond 1272* (F); Pat Sin Leng, Plover Cove Country Park, Plover Cove Reservoir, *S. Ickert-Bond 1266* (F). **Zhejiang**: Between Ping Yung and Tai Suan, *R.-C. Ching 2199* (E); Feng Yang Moutain, *H.-Y. Zou 151, 79* (MO), *762* (GH); Taishun Hsien, *Y. L. Keng 316* (GH); Yeshanling, Taishun, *Ickert-Bond 1379* (F).